Diplomarbeit

Upcycling von Polypropylen: Herstellung von Schäumen

ausgeführt zum Zwecke der Erlangung des akademischen Grades einer
Diplom-Ingenieurin (Dipl.-Ing. oder DI)
eingereicht an der TU Wien, Fakultät für Maschinenwesen und Betriebswissenschaften
von

Catherine THOMA

Mat.Nr.: 01026343 (066 434)

unter der Leitung von

Ao.Univ.Prof. Dipl.-Ing. Dr.mont. Vasiliki-Maria Archodoulaki

und

Projektass. Dipl.-Ing. Florian Kamleitner

E308 Institut für Werkstoffwissenschaften und Werkstofftechnologie

Ich nehme zur Kenntnis, dass ich zur Drucklegung meiner Arbeit unter der Bezeichnung

Diplomarbeit

nur mit Bewilligung der Prüfungskommission berechtigt bin.

Eidesstattliche Erklärung

Ich erkläre weiters Eides statt, dass die vorliegende Arbeit nach den anerkannten Grundsätzen für wissenschaftliche Abhandlungen von mir selbstständig erstellt wurde. Alle verwendeten Hilfsmittel, insbesondere die zugrunde gelegte Literatur, sind in dieser Arbeit genannt und aufgelistet. Die aus den Quellen wörtlich entnommenen Stellen sind als solche kenntlich gemacht.

Das Thema dieser Arbeit wurde von mir bisher weder im In- noch Ausland einer Beurteilerin/einem Beurteiler zur Begutachtung in irgendeiner Form als Prüfungsarbeit vorgelegt. Diese Arbeit stimmt mit der von den Begutachterinnen/Begutachtern beurteilten Arbeit übereinstimmt.

Wien, im Dezember 2017

_____

Catherine Thoma

Danksagung

„In jede hohe Freude mischt sich eine Empfindung der Dankbarkeit."

- Marie von Ebner-Eschenbach

An dieser Stelle möchte ich allen danken, die diese Diplomarbeit durch ihre fachliche und persönliche Unterstützung begleitet und zu ihrem Gelingen beigetragen haben.

Speziell gilt mein Dank Frau Ao.Univ.Prof. Dipl.-Ing. Dr.mont. Vasiliki-Maria Archodoulaki für die Bereitstellung des Themas und die angenehme Betreuung. Des Weiteren möchte ich mich bei Herrn Projektass. Dipl.-Ing. Florian Kamleitner bedanken, der mir bei praktischen Aspekten sowie bei allgemeinen Fragen zur Arbeit stets zur Verfügung stand. Mein Dank gilt auch Sampo Zoppoth für die vielen hilfreichen Tipps und die Bereitstellung der Daten der thermischen Analyse von Hydrocerol PEX 5024.

Anschließend möchte ich mich auch bei meinem Freund Dipl.-Ing Rosenfeld bedanken, der mich während meines Studiums immer motiviert und aufgeheitert hat.

Zuletzt möchte ich auch bei meinen Eltern und Geschwistern danken, die mich nicht nur während der Diplomarbeit, sondern auch während meines gesamten Studiums tatkräftig unterstützt und ermutigt haben.

Kurzfassung

Polymerschäume werden heutzutage durch ihre einzigartigen Eigenschaften, insbesondere ihrer niedrigen Dichte und Wärmeleitfähigkeit in vielen Anwendungsgebieten eingesetzt. Polypropylenschäume sind ein vielversprechender Ersatz für viele industrielle Anwendungen. Das hohe Potential wird allerdings durch die geringe Schmelzfestigkeit und die niedrige Schmelzelastizität eingeschränkt.

Die Arbeit ist Teil des Projekts „Innovatives Kunststoffen Up-Cycling“, dessen Ziel das „Upcycling“ von Polypropylen aus Nachgebrauchsabfall durch Langkettenverzweigung ist. Da die Schaumproduktion eine vielversprechende Nischenanwendung des recycelten Polypropylene ist, wurde in dieser Arbeit die Herstellung von Schäumen aus ausgewählten Thermoplasten mittels Schaumextrusion näher untersucht. Ziel dieser Arbeit war die Optimierung vom chemischen Schäumen im Einschneckenextruder um anschließend den Einfluss der Langkettenverzweigung auf die Schäumbarkeit zu ermitteln. Dazu wurden die optimalen Prozesseinstellungen und Prozessparameter für einen Einschneckenextruder ermittelt und in Vorversuchen das Schaumverhalten von Polystyrol und Polyethylen niedriger Dichte untersucht.

Es stellte sich heraus, dass die Düse und speziell auch die eingestellte Temperatur an der Düse den größten Einfluss auf die Schaumqualität haben. Aus diesem Grund wurde die ursprüngliche Düse des Extruders verlängert und der Querschnitt vergrößert.

Auch die Drehgeschwindigkeit der Schnecke und die Art des Schäumungsmittels beeinflusst das Schaumergebnis. Des Weiteren haben rheologische Eigenschaften, wie die Schmelzsteifigkeit und die Dehnverfestigung einen Einfluss auf den produzierten Schaum.

Es konnten die optimalen Prozessparameter für die Schaumextrusion mittels Einschneckenextruder gefunden und Schäume unterschiedlicher Thermoplasten hergestellt werden. Die Langkettenverzweigung verbessert die Schäumbarkeit von Polypropylen. Lineares Polypropylen wurde dazu mittel Reaktivextrusion mit einem Peroxydicarbonat (PODIC) langkettenverzweigt und mit einem chemischen Schäumungsmittel geschäumt. Dies alles erfolgte in einem einzigen Extrusionsschritt. Der hergestellte Schaum wurde mit dem Schaum einer kommerziellen HMS-PP Type und dem Schaum des linearen Polypropylens verglichen. Die erhaltenen Ergebnisse zeigten, dass die Langkettenverzweigung mittels Reaktivextrusion in Kombination mit chemischem Schäumen des Polypropylens eine vielversprechende Methode zur Schaumherstellung aus linearem Polypropylen ist.

Abstract

Foamed polymers are used in many applications due to their outstanding characteristics such as their reduced weight and thermal conductivity. A promising substitute in many industrial applications are polypropylene foams. Unfortunately, their high potential is limited by the low melt strength and melt elasticity.

This thesis is embedded in the project “innovative polymer upcycling”, which focuses on the up-cycling of polypropylene from post-consumer waste by long chain branching. As the foam industry is considered as an application sector, the focus of this thesis is on the foam production by foam extrusion of selected thermoplastics, such as polypropylene. Therefore, the optimal processing conditions and process parameters for a single screw extruder set-up were determined and preliminary studies of the foamability of polystyrene and low-density polyethylene were conducted.

The die temperature had the greatest impact on the foam quality, followed by that of the screw speed and the type of chemical foaming agent. The original die of the single screw extruder was extended with an additional forming section for this reason. Rheological properties, such as high melt strength and pronounced strain hardening also had an influence on the produced foam.

The optimal processing conditions for an extrusion foaming process were found and foams of various thermoplastic resins were produced. Long-chain branching of polypropylene improved its foamability. Additionally, a linear polypropylene was long-chain branched by reactive extrusion with peroxydicarbonate (PODIC) and foamed with a chemical blowing agent in one step. The produced foam was compared to a long chain branched polypropylene foam from a commercial high melt strength polypropylene and the foam of the linear polypropylene resin. The foaming with PODIC and a chemical blowing agent proved to be a promising method for the production of polypropylene foams from linear polypropylene resins.

Contents

1 Introduction

1.1 Aim of the thesis

The aim of the thesis is to analyse the foamability of various thermoplastic resins, more accurate those of linear polypropylene and long chain branched polypropylene.

It is therefore necessary to determine the optimal processing conditions and process parameters which have an influence on the foam quality. Polystyrene and low-density polyethylene are foamed to investigate the possibilities and limitations of the single screw extruder set-up.

The foamability of linear polypropylene is compared to those of two commercially traded high melt strength (HMS) polypropylene resins. An essential task of this thesis is also the long chain branching and foaming of linear polypropylene in one step by reactive extrusion with peroxydicarbonates and a chemical blowing agent.

The thesis is divided into three parts. The first part describes the theory of polymer foaming, more specific those of polymer extrusion foaming. It should give a short overview of the influence of various processing parameters and provide a link between the processing behaviour, the molecular structure and the rheological properties of the thermoplastic resins. The second part shows the experimental set-up and contains information about the used materials. It also defines the methods of data gathering and evaluation of thermal analysis and rheological measurements as well as the characterisation of the foam morphology. In the third part of the study, the evaluate data will be explained and discussed.

The Vienna University of Technology dedicated a lot of research on an innovative up-cycling process of polypropylene post-consumer waste. Recent studies consider long-chain branching of polypropylene as a promising approach to improve the melt strength of polypropylene and consequently improve the quality of the produced foam [1, 2].

2 Theoretical Background

A foam is defined as gaseous voids that are surrounded by a much denser matrix. The classification of foams is usually either by density (high, medium, low), dimension (e.g. board, sheet), structure (open, closed cells), cell size (e.g. nano-, microcellular) or nature (flexible, rigid). As can be seen in Figure 1 many different applications from furniture to packaging have been established for polymeric foams [3].

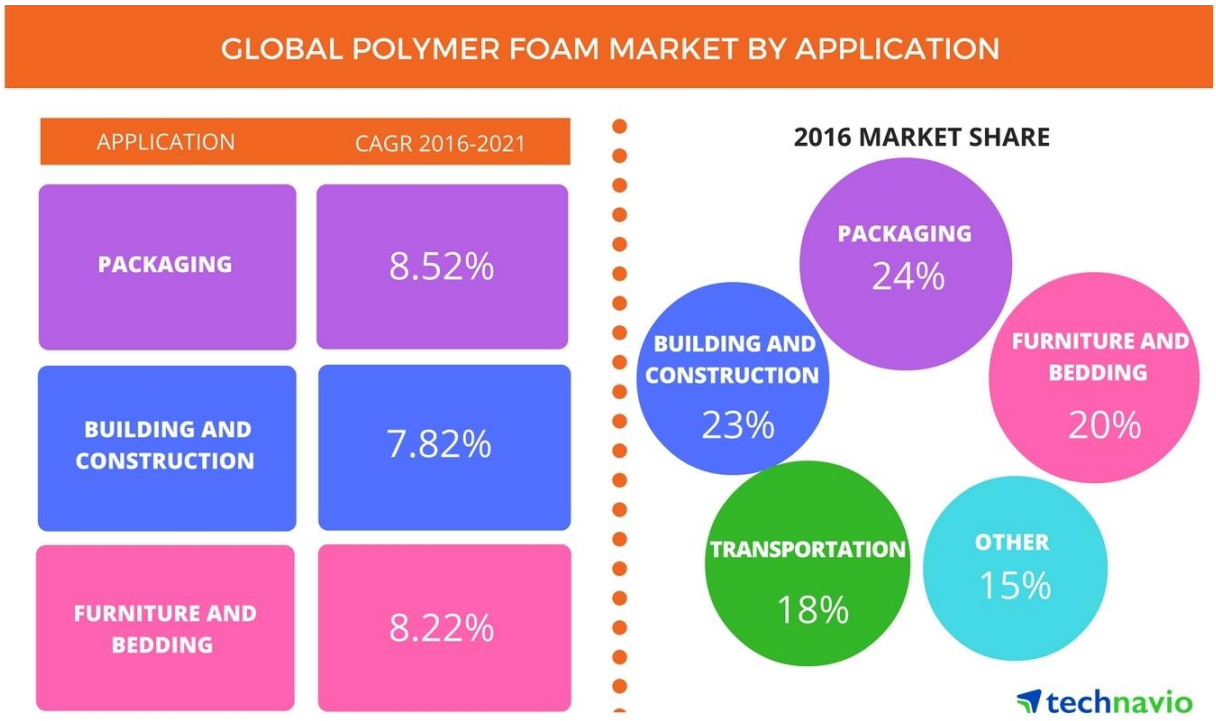

Figure 1: Global polymer foam market by application [4]

Polymer foams possess outstanding characteristics that make them unique in comparison to unfoamed polymeric materials and enable them to be used efficiently for various industrial applications. Advantages of polymeric foams include a reduced weight, energy absorbtion and low thermal conductivity to name a few. Polyolefin foams also keep the properties of the polyolefin such as toughness, flexibility and resistance to chemicals and abrasion. According to a report by Marketsand Markets, the global polymer foam market is forecast to rise at an annual growth rate (CAGR) of ~6% in 2017 and 2022. A market study by Technavio even estimates an annual growth rate of more than 8% until 2021. The rising growth rate is pushed by the demand of the automobile, construction and packaging industries as well as various others. Asia, Europe and North America are predicted to become the world's largest polymer foam markets [4, 5, 6, 7].

An analysis of Europe's plastic demand in 2015 lists polypropylene on second place with 19.1% and low-density polyethylene on third place with 17.3% respectively. The demand for polystyrene is 6.9%. Polystyrene is an easy-to-foam material. Polypropylene foams have been considered as a substitute in industrial application due to their low material cost and promising

material properties such as its higher rigidity and strength than polyethylene and a better impact strength than polystyrene. The higher service temperature is also an asset. Unfortunately, polypropylene is limited due to its weak melt strength and melt elasticity [8, 9].

2.1 Polymer foaming

There are three main steps in the foam process (see Figure 2) [8, 10]:

1. Dissolving of the gas in the polymer melt
2. Cell nucleation
3. Cell growth and stabilisation

The gas can either be directly injected into the polymer melt (physical blowing agent) or is formed by decomposition of a chemical blowing agent. The generation of gas is influenced by the momentum and heat transfer as well as the Non-Newtonian behaviour of the melt. The formation of the cells is influenced by micro voids and/or a nucleation agent. These function as nucleation sites. The initial growing mechanism of the created bubbles is either driven by the diffusion of gas from solution into the bubbles, or by expansion due to heat or pressure reduction. The cell growth continues until the bubble is stabilised or ruptures. It mainly depends on the temperature, the hydrostatic pressure, the state of supersaturation and the viscoelasticity of the polymer gas solution [8, 10, 11].

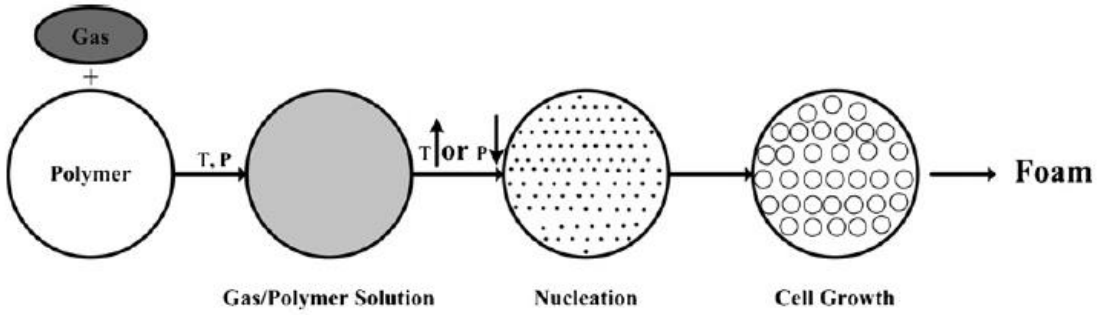

Figure 2: Main steps of the foam process [12]

Cells may also grow by the combination of two or more bubbles. This process, also called coalescence (see Chapter 2.6), occurs due to the reduction of the free energy of the polymer melt/ gas system. It is also caused by the shear field in the die, which stretches the nucleated bubbles and consequently accelerates cell coalescence. In order to overcome this phenomenon, it is necessary to take the rheological behaviour into account. The melt strength is determined by shear and extensional flow. It can be defined as a degree of resistance to the extensional flow of the cell walls and thus is an important property in suppressing cell coalescence. Increasing the melt strength helps to suppress cell coalescence by increasing the cell wall stability. Reducing the die temperature and controlling the pressure in the die are important parameters in this context as well. Another apparent issue in the foam process is that fewer cells are more stable in a system for a given foam volume. At equilibrium, the pressure in a spherical bubble

is higher than in the surrounding fluid. The gas pressure in smaller bubbles is larger than in bigger ones. This leads to the diffusion from smaller bubbles to larger ones and consequently to a decrease of the foam density. Rheological properties, such as melt strength and shear viscosity, also maintain the high pressure and avoid premature nucleation [11, 13, 14, 15, 16].

Too rapid expansion of the cells which causes the rupture of the cells is also problematic. This results in the collapse of the foam structure after it exits the die. This problem can be overcome by lowering the melt temperature, which increases the melt viscosity, allowing the structure to stabilise. The cell growth and rupture strongly depend on the rheological properties, e.g. elasticity. Strain hardening, which is an extensional behaviour of the melt, helps to stabilize the bubble structure. It induces a so-called self-healing effect, which causes a more homogeneous deformation of the melt under extensional flow [11, 13, 16, 17, 18].

The main parameters that have a direct influence on the nucleation and growth of cells are the type and initial concentration of the blowing agent, the distribution of the pressure in the melt and the solubility and diffusivity of the gas [16].

Basically, there are four main processes to produce polymer foams [19, 20]:

1. Particle foams
2. Multi-component plastic foam
3. Thermoplastic injection moulding
4. Foam extrusion

Particle foams, also known as expanded foams are made in a two-step process. First the polymer into which the foaming agent is mixed, is pre-foamed. The pre-foaming of the thermoplastic material inflates the volume to 20-50 times of its original size. The pre-foamed thermoplastic material is then formed into blocks, panels or other shaped elements. The most common known particle foam is EPS (expanded Polystyrene), which is used as insulation material [21].

Polyurethane foam (PU-foam) is a typical member of multi-component plastic foams, which are produced by the reaction of two or more components. The polyurethane is formed by a reaction known as addition polymerization of the chemical precursors isocyanate and polyalcohol. The formed CO_2 acts as blowing agent. The use of n-Pentane as blowing agent is widespread in Europe as well [19, 22].

Thermoplastic foam injection moulding and foam extrusion can either be performed by using a physical or a chemical blowing agent (see Chapter 2.2.1 and 2.2.2). By using a physical blowing agent, the polymer melt is mixed with the gas. After exiting the die, the polymer-gas dispersion is forced into a mould cavity, where the actual foaming process begins. The gas expansion and cell growth are mainly governed by the pressure in the mould cavity. In contrast to the injection foam moulding, the gas expansion in the foam extrusion process depends on the atmospheric pressure. As a result, a higher volume expansion ratio can be achieved [20, 23].

Foam extrusion has been the largest sector in thermoplastic foam industry since it has been introduced [19, 20].

2.2 Foam extrusion process

In the direct extrusion foaming process of a thermoplastic, a gas is dispersed and homogenized in the fluid polymer phase. This technique is called dispersion principle. It is based on the saturation of the polymer melt with a gas under pressure. The reduction of the pressure or the increase of temperature causes the foaming of the material [13, 24].

An extruder can be divided at least in the following three sections as can be seen in Figure 3: Feed section, compression section, metering section [3, 17, 20].

- The primary task of the feed section is to get the polymer in contact with the screw, therefore the polymer is gravity fed into the barrel of the extruder by a hopper. At the feed throat, there is usually a water cooling device to prohibit the polymer from foaming out of the hopper. Through the rotation of the screw the polymer is led further into the heated barrel.
- In this compression section the polymer is completely melted or plasticized and mixed. To achieve an adequate mixing the dwell time of the polymer melt is important. Only about 50% of the energy needed to melt the polymer is contributed by the heating system, the additional energy input comes from friction and the intense pressure inside the barrel.
- In the metering section the polymer melt is further homogenized. In a single screw extruder, this is also the section in which the gas is formed in the polymer melt. The pressure also increases in this section. The polymer melt then enters the breaker plate and the die. The design of the die creates a high-pressure gradient, keeping the gas compressed in the die and consequently preventing premature foaming. After the die exit the sudden decrease in the pressure allows the gas to expand and in doing so creating the foam. The final shape of the product is influenced by the shape of the die.

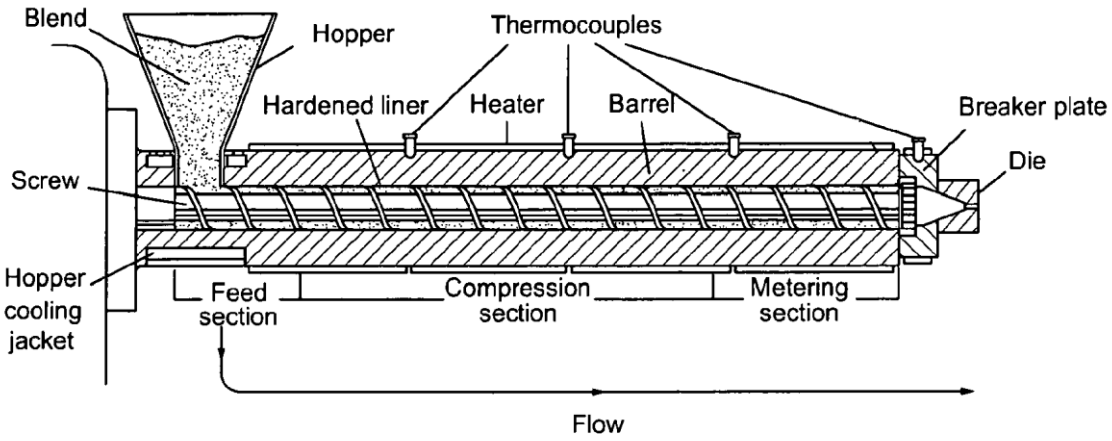

Figure 3: Single screw extruder [25]

2.2.1 Physical foaming

Physical blowing agents (PBA) liberate gases because of a physical process, e.g. evaporation or desorption at higher temperatures or reduced pressures without a chemical reaction. Above the low, pressure dependent boiling point they evaporate, causing a volume expansion, that expands the polymer mass [24, 26].

The PBA's are usually injected at approximately 2/3 of the way between the feed throat and the die of the single screw extruder using either a vent port or a tandem extruder configuration [17]. A scheme of a tandem extruder configuration is shown in Figure 4.

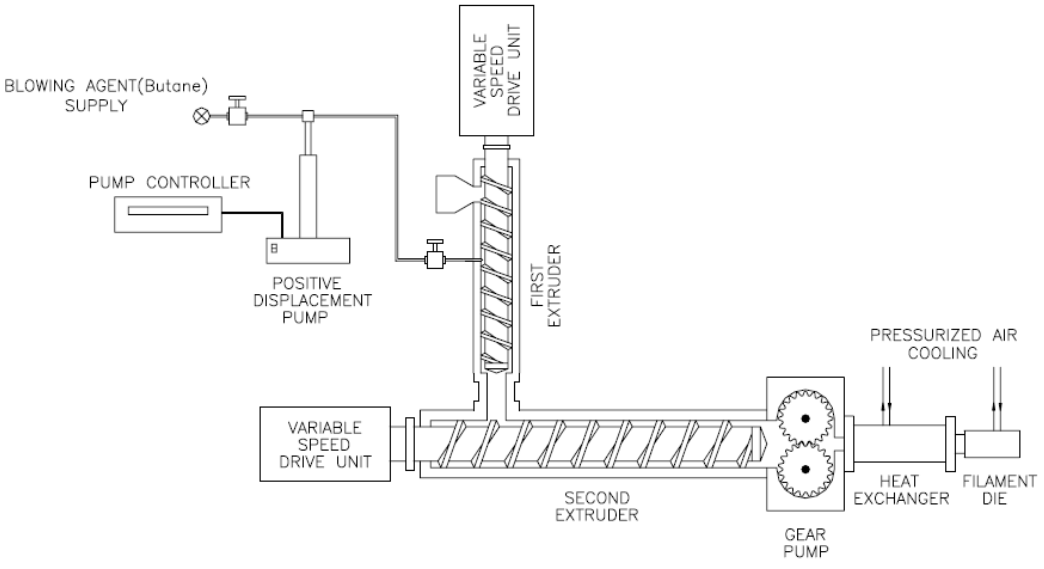

Figure 4: Tandem extruder configuration [27]

The first extruder is used for the plasticisation of the polymer, while the second extruder is used for intensive mixing. Additionally, it functions as heat exchanger. The production rate capacity is often limited by requirements for cooling, mixing and a limited surface area for heat extraction. To overcome these limitations a second extruder is designed to optimize the extraction of heat and to guarantee an optimal processing temperature by reducing the melt temperature to a suitable range for the foam production [3].

2.2.2 Chemical foaming

Chemical blowing agents (CBA) decompose at a specific temperature and thereby generate a gas, which then forms the cell structure. They can be mixed with the polymer and then be fed to the hopper. The smaller the particle size of the CBA, the faster it decomposes. Whether the decomposition temperature of the CBA is reached, depends on the temperature range of the extrusion process as well as on the residence time. Higher temperatures of the polymer melt lead to a faster decomposition. However, adding an activator can reduce the decomposition temperature significantly. Nevertheless it is necessary to melt the polymer at a temperature below the decomposition temperature, before increasing the temperature in the barrel and starting the decomposition of the CBA [17].

The selection of the appropriate blowing agent depends on the decomposition temperature and the type of gas that is generated. Generally, there are two types of chemical blowing agents, exothermic and endothermic ones. Exothermic CBA's generate heat, while endothermic CBA's absorb it. Exothermic CBA's have a rapid decomposition in a narrow temperature range, resulting in a decomposition that once started, is difficult to stop. Endothermic CBA's stand out due to their broader decomposition temperature and time range. Another difference is that exothermic CBA's usually produce N_2, while endothermic ones produce mainly CO_2 as the main blowing gas. This can be seen from the properties provided in Table 1 [28].

Table 1: Properties of chemical blowing agents [29]

Description	Type	Decomposition temperature [°C]	Gases
Azodicarbonamide (ADC)	Exo	200-230	N_2, CO, NH_3, O_2
4,4-Oxybis(benzenesulfonylhydrazide) (OBSH)	Exo	150-160	N_2, H_2O
p-Toluenesulfonylhydrazide (TSH)	Exo	110-120	N_2, H_2O
p-Toluenesulfonylsemicarbazide (TSS)	Exo	215-235	N_2, H_2O
Sodiumbicarbonate	Endo	120-150	CO_2, H_2O
Citricacidderivatives	Endo	200-220	CO_2, H_2O

PBA's are widely used to make a low-density foam without crosslinking, whereas for low density foam processing involving crosslinking, CBA's are favoured. Typically, CBA's are also used to produce medium to high density foams in a range of 400-800 kg/m^3. The density reduction achieved with chemical blowing agents is significantly lower than those of physical blowing agents [8, 30].

2.3 Thermoplastic materials

Thermoplastics are made of long, polymer chains. They can be heated and reshaped into a specific design and then cooled and solified. This process is also reversible, which is an important aspect in the recycling of thermoplastics. The different types of thermoplastics vary amongst other things in their chemical structure, their crystallinity and their density. Semi-crystalline polymers show a melting temperature, at which they change from solid to liquid state, as well as a glass transition temperature. The glass transition temperature marks the temperature at which they transfer from a hard and brittle state to a viscous state. Amorphous polymers only have a glass transition temperature. Commonly produced thermoplastics are polystyrene, polyethylene and polypropylene [31].

Amorphous polymers, like polystyrene have the largest processing window, as can be seen in Figure 5. They also can be cooled more before exiting the die. Polyethylene has a smaller processing window, followed by that of polypropylene [17].

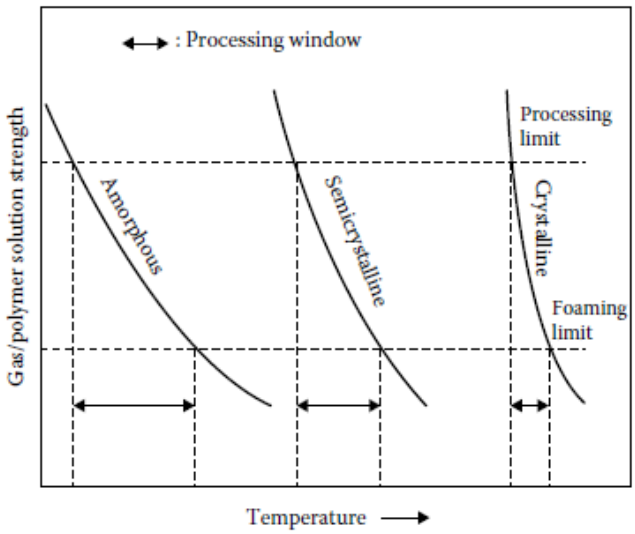

Figure 5: Processing window of amorphous, semi crystalline and crystalline thermoplastics [17]

2.3.1 Polystyrene

Polystyrene (PS) is depending on tacticity either an amorphous or a semi crystalline thermoplastic. In atactic polystyrene the phenyl substitutes have randomly placed positions along the chain length. Atactic polystyrene has an amorphous structure due to their random structure and the missing formation of crystalline regions. It has a glass transition temperature

of about 100°C. Isotactic Polystyrene is a semi crystalline polymer with all the substitutes located on the same side of the macromolecular backbone. The melting temperature of isotactic polystyrene is $T_m \cong 230°C$. The chemical structure of polystyrene is given in Figure 6 [31].

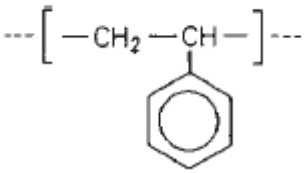

Figure 6: Chemical structure of polystyrene [31]

A higher die temperature leads to an increased number of pores in the produced polystyrene foam and changes the morphology of the pores to almost spherical at 220°C. It has been shown that coalescence and growth phenomena of cells occur with rising temperature, leading to a larger porosity and therefore a decreased expansion [32].

The materials properties, such as toughness, transparency and brittleness, are determined by its structure. It also causes the high temperature dependency of the viscosity. The viscosity increases rapidly with decreasing temperature. The melt elasticity of polystyrene is due to its rigid structure lower than e.g. that of branched low-density polyethylene [31, 33].

2.3.2 Low-density Polyethylene

Polyethylene (PE) is often classified by density. Figure 7 shows the most common types of polyethylene and the chemical structure of this polymer. The different types of PE also vary in their number and type of branching. Those characteristics also influence properties, like crystallinity or density. Polyethylene has a high ductility and elongation at break [31].

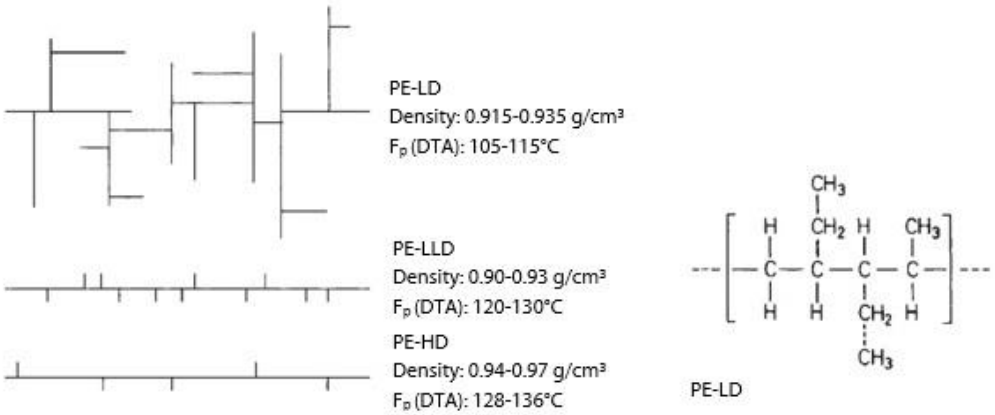

Figure 7: Common types of polyethylene (left) and chemical structure (right) [31]

Low-density polyethylene (LDPE) has a lower melt temperature than high-density polyethylene (HDPE) and linear low-density polyethylene (LLDPE). Typical values for the melt temperature and the density are given in Figure 7. Neither HDPE nor LLDPE have the long-branched molecular structure and melt strength of LDPE. Both are essential criteria for an optimum foam process [34].

2.3.3 Linear Polypropylene

Polypropylene (PP) consists of highly linear chains and a narrow molecular weight distribution. The crystallinity and the grade of crystallinity are also dependent on tacticity. A high crystallinity can be found in isotactic polypropylene due to the regular positions of the methyl group (CH_3). Isotactic polypropylene has the highest melt temperature ($T_m \cong 185°C$). In syndiotactic polypropylene the substitutes have alternate positions along the chain, its melt temperature is ~161°C. Atactic polypropylene is an amorphous polymer. The chemical structure of PP with different tacticity is given in Figure 8 [31].

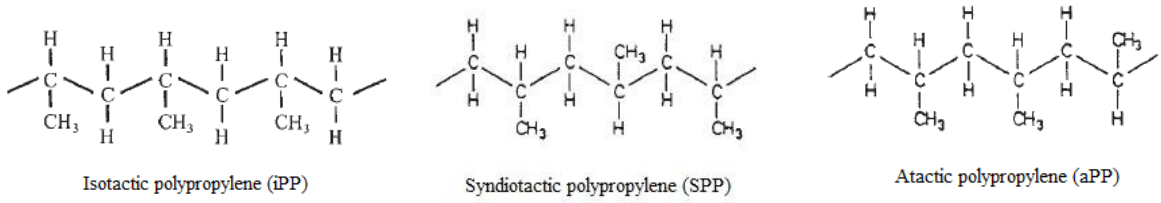

Figure 8: Chemical structure of polypropylene with different tacticity [31]

Polypropylene is difficult to foam because of its rheological properties, especially its low melt strength. This causes the cell walls, which separate the bubbles, to be too weak to bear the extensional force. They are likely to coalescence and rupture, producing a high open cell content. When the barrel temperature is higher than the melt temperature, the melt strength and the viscosity decrease rapidly. This affects the stabilisation of the cell structure [17].

They also do not show strain hardening (Chapter 2.4.2). To lower the melt viscosity of PP during extrusion, it is more effective to increase the shear rate than the melt temperature. PP is a shear sensitive polymer, a change in temperature only has a minor effect on the melt viscosity [35, 36].

2.3.4 Long chain branched Polypropylene

Long chained branched polypropylenes (LCB-PP) have a higher elasticity, a more pronounced shear thinning, and a significant strain hardening compared to linear PP. Often the commercial name is high melt strength polypropylene (HMS-PP). Strain hardening induces a so-called self-healing effect leading to a more homogeneous deformation of the melt under elongational flow as it occurs during cell growth. It has been shown that LCB-PP foam has a higher volume expansion ratio, a suppressed cell coalescence and a more homogeneous cell structure. The melt strength and the degree of strain-hardening increases with an increasing number of long chain branches [36, 37].

Long chain branching also increases the molar mass and broadens the molar mass distribution. Several methods of LCB formation are reported in literature. A promising approach particularly with regard to foam extrusion of polypropylene is long chain branching by reactive extrusion with peroxydicarbonates (PODIC). A reaction scheme of LCB-formation assisted by PODIC with long aliphatic side chains is given in Figure 9 [1, 2, 38].

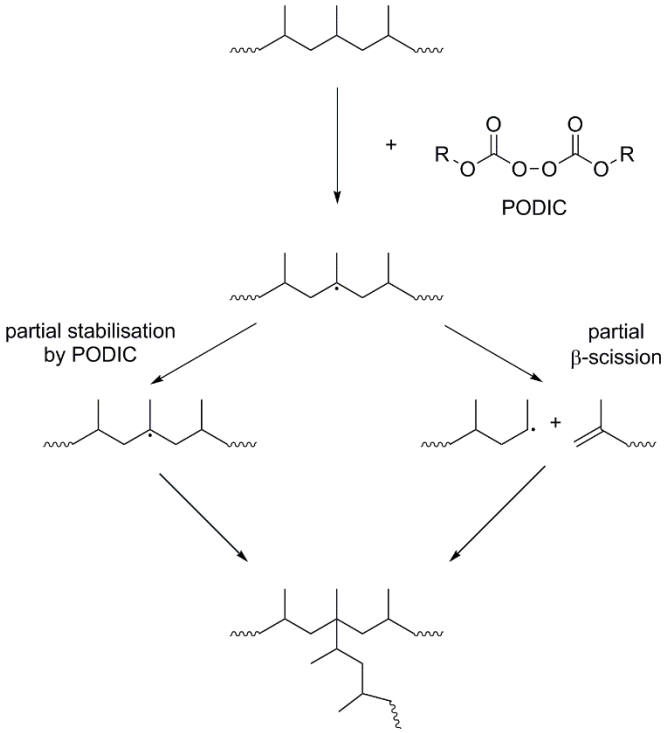

Figure 9: Reaction scheme of LCB formation with PODIC [2, 38]

The first step of the LCB formation is the radical induced activation of the PP backbone. In the reactive extrusion with peroxydicarbonates, the PODIC acts as peroxide to generate radicals. The further processes are a combination of partial chain scission and recombination. Recent studies have shown that in reactive extrusion of PP with PODIC a higher molar mass leads to a much more pronounced chain scission than recombination reaction. The PODIC itself also acts as stabilizing agent and consequently enhances a successful recombination and long chain branching [1, 2].

2.4 Rheological parameters

Rheology is defined as the science of deformation and flow of materials. The rheological parameters are the link between the processing behaviour and the molecular structure of the resin (Figure 10)[19, 39].

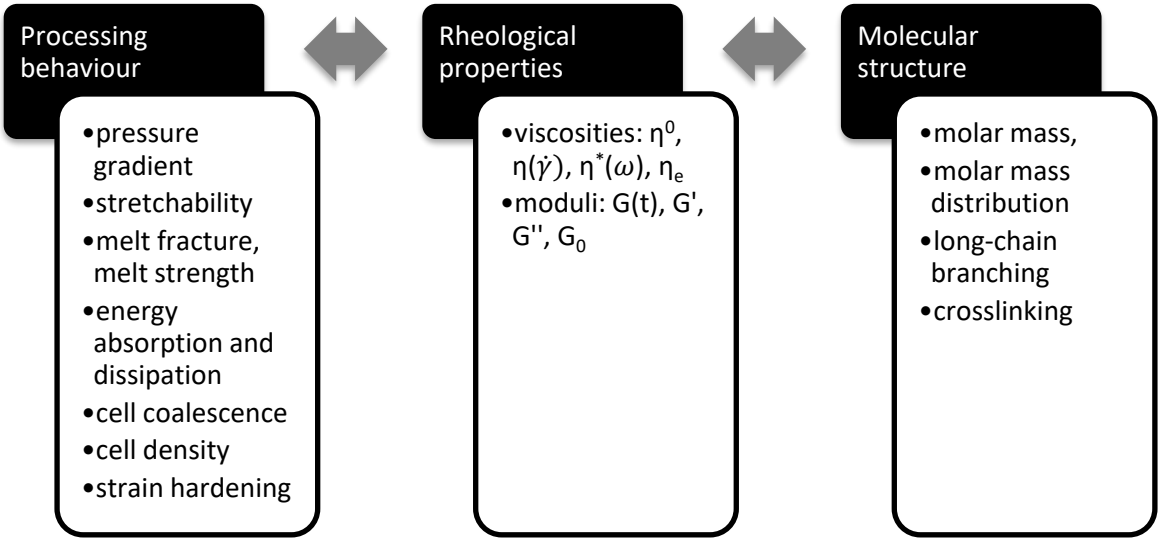

Figure 10: Link between the rheological properties and the processing behaviour and molecular structure [39]

Many Polymers, esp. those used in this thesis, show a pseudo-plastic behaviour also known as shear thinning. At low shear rates the viscosity is independent of the shear rate, this corresponds to a Newtonian Fluid behaviour. With an increased shear rate, e.g. by a faster extrusion, the viscosity decreases due to molecular alignments and disentanglements of the long chains. This is shown in Figure 11 [19, 37].

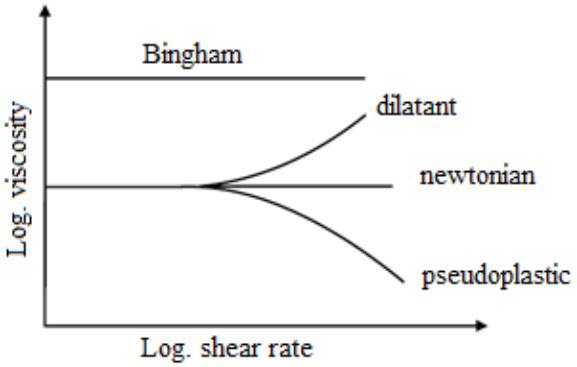

Figure 11: Classification of common flow behaviours [19]

Shear thinning is caused by molecular alignments and disentanglements of the long polymer chains. At very high shear rates melt fracture occurs. Melt fracture is a flow instability. The

rheological properties are linked to the process conditions and the molecular structure of the polymer resin. The effect of selected properties on the viscosity are given in Figure 12 [19].

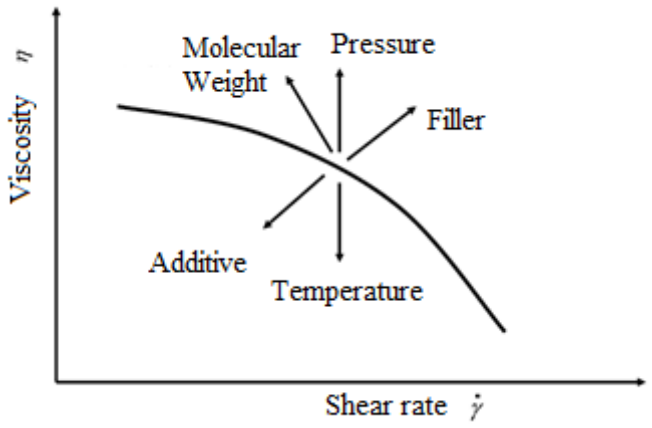

Figure 12: Influence of various parameters on viscosity [19]

2.4.1 Shear viscosity

Shear viscosity can be easily derived from dynamic measurements [19]. The polymer is therefore imposed to a sinusoidal stress on a parallel plate rheometer (Figure 13).

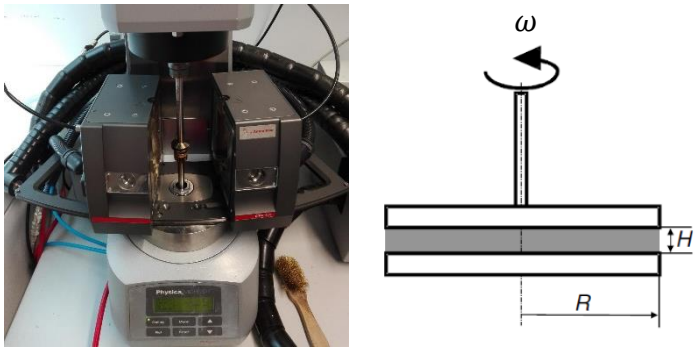

Figure 13: Parallel plate rotational viscometer [19]

For an ideal elastic material, the stress σ can be set as the product of the modulus G and the strain ε. For a Newtonian fluid the strain rate $\dot{\gamma}$ must be considered as well. A polymeric fluid shows viscoelastic behaviour, so it will be out of phase. The dynamic measurements determine the complex modulus, consisting of the storage and the loss modulus, as well as the complex viscosity [19].

The storage modulus and the loss modulus can be defined as [19]:

$$\text{Storage modulus } G'(\omega) = \frac{in\text{-}phase\ stress}{max.strain} \qquad \text{Eq. 2-1}$$

$$\text{Loss modulus } G''(\omega) = \frac{out-of-phase\ stress}{max.strain}$$

Eq. 2-2

The storage modulus gives the elastic response of the polymer, while the loss modulus is the viscous part. A higher storage modulus *G'* implies a higher elasticity. The course of the storage modulus *G'* over the frequency of oscillation ω shows if a sample has a narrow or a broad molecular weight distribution. The crossover point *G'* = *G''* can be used to estimate the polydispersity M_w/M_n [19].

The complex viscosity $|\eta^*|$ is calculated from the dynamic viscosity with the given formulas.

$$\eta' = \frac{G''}{\omega} \quad or \quad \eta'' = \frac{G'}{\omega}$$

Eq. 2-3 or. Eq. 2-4

$$|\eta^*| = \sqrt{\eta'^2 + \eta''^2}$$

Eq. 2-5

The Cox-Merz rule states that the steady-state shear viscosity η is equal to the complex viscosity.

$$|\eta^*(\omega)| = \eta(\dot{\gamma})$$

Eq. 2-6

The shear viscosity affects various processes inside the foam extrusion line, e.g. the extrusion rate, the dispersion of the blowing agent and the pressure inside the die. Except for the die pressure a low viscosity is favoured. The shear viscosity of the polymer melt is reduced by mixing the blowing agent and the melt due to the plasticisation of the polymer melt. Figure 14 shows typical processing shear rates. Shear rates for extrusion processes range from 50 s^{-1} to several 100 s^{-1} [40, 41].

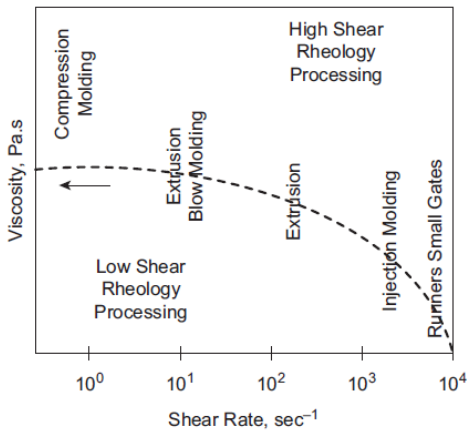

Figure 14: Processing shear rates [41]

2.4.2 Extensional viscosity and melt strength

The extensional viscosity η_E^+ is defined as the resistance of a fluid to extension. It determines the bubble stability during the foam extrusion outside the die [40].

Extensional viscosity can be measured with rheometers by applying extensional stress. Typical values for strain rates are 0.1 s^{-1}, 1 s^{-1} and 10 s^{-1}. The extensional flow during the bubble growth has strain rates in the range of 1 s^{-1} to 5 s^{-1}. The start up curve for the extensional viscosity can be obtained from Trouton's ratio (TR). Trouton's ratio (Eq. 2-7) gives the ratio of the extensional viscosity and the shear viscosity. It is equal to 3 for a Newtonian fluid. At low shear rates and uniaxial elongation this is also valid for pseudo plastic fluids like polymers [3, 42].

$$TR = \frac{\eta_E(\dot{\varepsilon})}{\eta(\dot{\gamma})} = 3$$

Eq. 2-7

Figure 15 shows two typical curves of a linear polymer and a long chain branched polymer. The linear polymer shows no deviation from the start up curve and consequently no strain hardening. The long chain branched polypropylene has by comparison significant strain hardening.

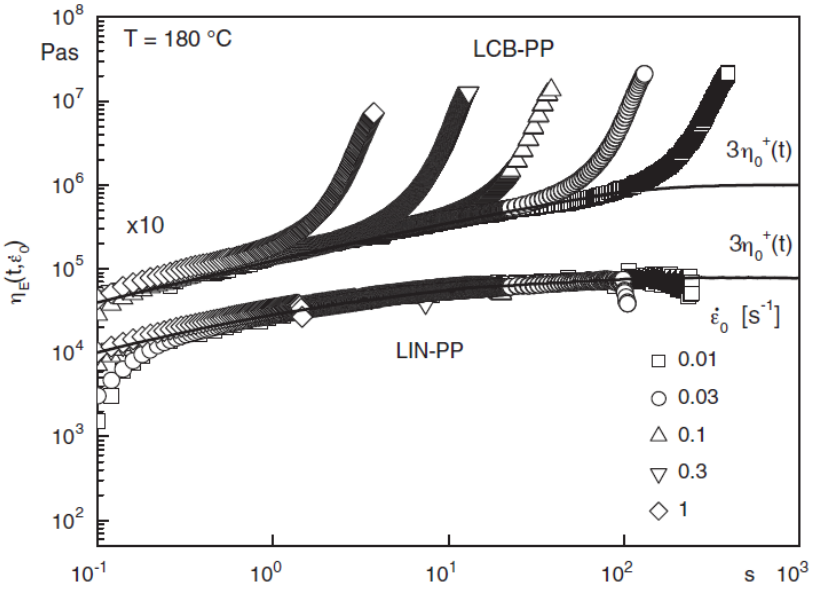

Figure 15: Viscoelastic start up curve η_E for a linear polymer LIN-PP and a long chain branched polymer LCB-PP at various strain rates at 180°C [43]

Melt strength

The melt strength is the force that is required to break the extruded strand [42].

Increasing the melt strength helps to suppress cell coalescence by increasing the cell wall stability. The melt strength can be increased by lowering the temperature. Other factors that enhance melt strength are branching, cross-linking, molecular weight and molecular weight distribution as well as blending of polymers [15].

2.5 Processing conditions and process variables

The foaming process is quite complex because the key variables (viscosity, glass transition temperature, surface tension, gas solubility and diffusivity) are all functions of temperature, pressure and gas content [44].

2.5.1 Screw speed

The screw speed is critical in controlling several tasks and parameters, e.g. mixing and melting, pressure generation, melt temperature and residence time in the extruder. On the one hand, a higher screw speed increases the melt temperature, provides greater mixing and puts more work into the polymer melt, but it also increases the resin degradation due to thermal energy. On the other hand, a lower screw speed provides a longer residence time in the extruder, a higher torque and screw fill. A higher screw speed provides a higher pressure drop at the die exit. The decomposition of endothermic blowing agents, like sodium bicarbonate, that have a slow decomposition rate over a broad temperature range, are affected by the shorter residence time [35, 45].

The dispersion and/or distributive mixing needs excessive work. The shear generates heat, which depending on the polymer might cause resin degradation. If the screw speed is too high, it might also cause so much shear heat, that it gets hard to control the melt temperature. Also shear thinning is more pronounced at high screw speeds, leading to a reduction of the melt viscosity and by that increasing the probability of cell rupture [35, 45].

2.5.2 Temperature profile

The temperature profile in the extruder is especially important in reducing the amount of gas loss. The cell wall decreases as the foam expands, allowing the diffusion rate of gas to increase even more. Preventing the diffusion through the extrudate skin is necessary to produce low-density foams. The lower the temperature, the lower is the diffusivity of the gas. One way of promoting large volume expansion is therefore to freeze the foam skin by lowering the die temperature. A basic strategy for this purpose is the use of a cooling device before the polymer melt with the dissolved gas passes through the die [8, 46].

By reducing the melt temperature, the stiffness of the melt increases. If the melt temperature is too low, the cell walls become too stiff and prohibit the foam to expand. As can be seen in Figure 16, this can affect the timing of the crystallization, delaying the cell growth at the beginning and leading to a stop of the cell growth in the foaming process due to too rapid crystallization. To achieve a maximum volume expansion ratio, the timing of the crystallization is essential. The dissolved gas has to diffuse into the nucleated cells and the foam should expand to its maximum capacity before the crystallization occurs [8, 46].

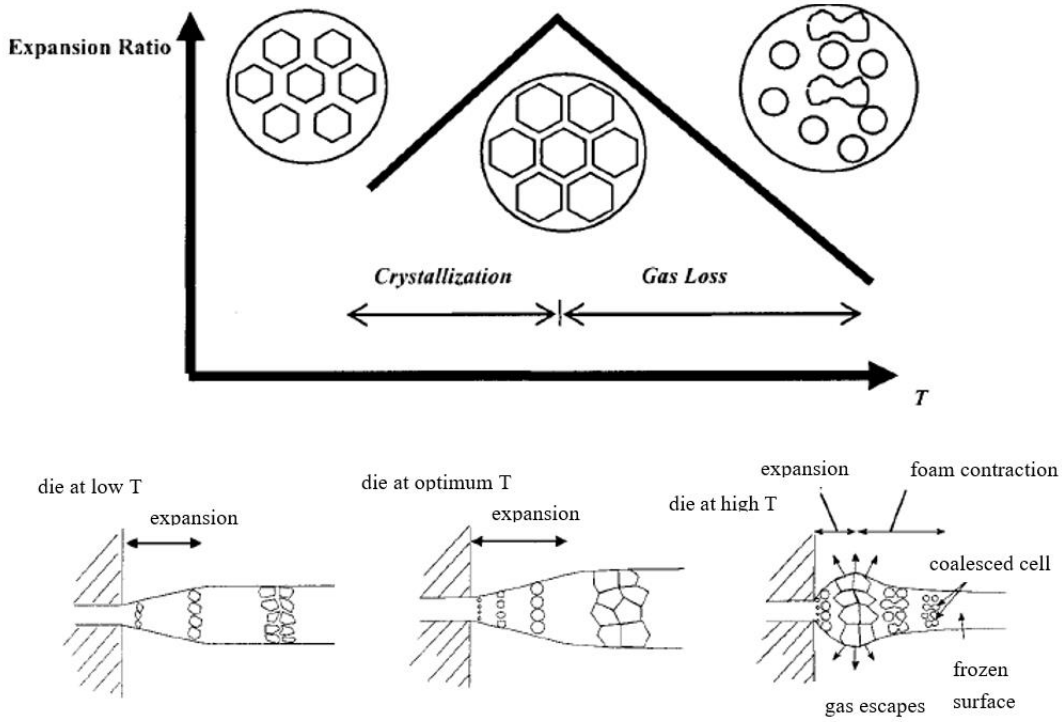

Figure 16: Main mechanisms that govern the expansion ratio [47]

Consequently, the volume expansion ratio is either governed by the loss of gas that escapes through the skin of the foam at high temperatures or by the crystallization of the polymer at low temperatures. This is visualised in Figure 16 [46].

2.5.3 Die pressure and die geometry

The expansion ratio is mainly governed by the flow rate, the die temperature, the die pressure and the pressure drop rate. The die pressure decreases with increasing die temperature due to the increased viscosity. The die pressure is a function of the screw speed, the type and amount of blowing and nucleation agents, the melt temperature, the die temperature and the die geometry [6, 16, 45].

Lee et al. [46] have shown within the same die groups (=group of dies with different geometry, that have either the same die pressure or the same pressure drop rate) the effect on the nucleation and the expansion behaviour is negligible as long as the die pressure stays above the solubility pressure of the gas. So, the die geometry itself does not influence the foaming behaviour. Their experiments have been carried out with polypropylene and CO_2 as physical blowing agent. Cell density and volume expansion ratio increase with increasing die pressure drop rate [46].

2.5.4 Blowing agent

Amount of blowing agent

In case of polypropylene an increasing amount of blowing agent decreases the foam density, but the rates of density change also depends on the polymer type. This is visualised in Figure 17. The amount of gas decomposition for a given CBA is dependent on the resistance time and the temperature [45].

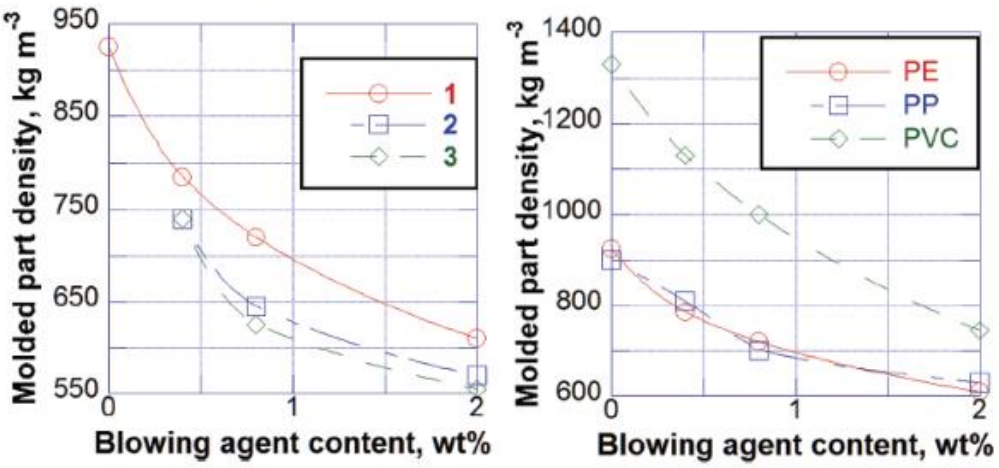

Figure 17: Effect of the amount of blowing agent on the foam density; left: foam density of polyethylene with different content of various blowing agents (1: Hostaron P1941; 2: Hydrocerol PLC751; 3: Adcol blow x 1020); right: foam density vs. content of Hostatron P 1941 with different polymers [45]

The expansion ratio can be quite effectively influenced by keeping the amount of blowing agent constant but rising the amount of nucleation agents like talc. The amount of blowing and nucleation agents not only affect the expansion ratio, but also the number of cells, the cell density and cell size as well as the thickness of the skin [45].

Dispersion and solubility of blowing agent

As the particle size of the blowing agent decreases, the surface area increases, leading to a faster decomposition rate. The finer the dispersion of the blowing agent in the polymer melt, the better the cell density and foaming process. The complete dispersion of the blowing agent, especially when dealing with azodicarbonamide, is not easy because agglomeration tends to occur. This problem is mostly addressed on the manufacturing level of blowing agents. The different sizes of the particles and the formation of agglomerates affect the decomposition rate. In addition agglomerated and undispersed particles produce voids and large gas pockets after the expansion, and therefore reduce the quality of the foam [48].

2.6 Cell coalescence

Pressure drop rate and shear stress are the main effects governing the cell nucleation of PS, when the saturation pressure or the amount of CBA is too low. The fast-flowing core region is mainly governed by the high pressure drop rate, while the slow flowing surface region is nucleated by the shear stress. The low pressure drop rate caused by the shear stress enhances cell nucleation, leading to a higher cell density at the surface region [6].

The shear field generated during the shaping process in the die deteriorates the nucleated cells while they are growing. This accelerates cell coalescence. The suppression of cell coalescence in the extrusion process is essential in guaranteeing the quality of the produced foam. This can be achieved by lowering the die temperature and thus increasing the melt strength [15].

3 Methodology and experimental set-up

3.1 Experimental set-up

The experiments were performed with a single screw extruder. The original extrusion set-up was modified by adding an additional forming section, which extends the die. The whole set-up consists of four main sections. The feeding section (S1), the melting and compression section (S2), the metering section (S3) and the forming section (S4). The feeding, the melting and the metering section have a heating system. S1 and S2 also have a cooling system. An annular die was used for the foam production. An image of the set-up is provided in Figure 18.

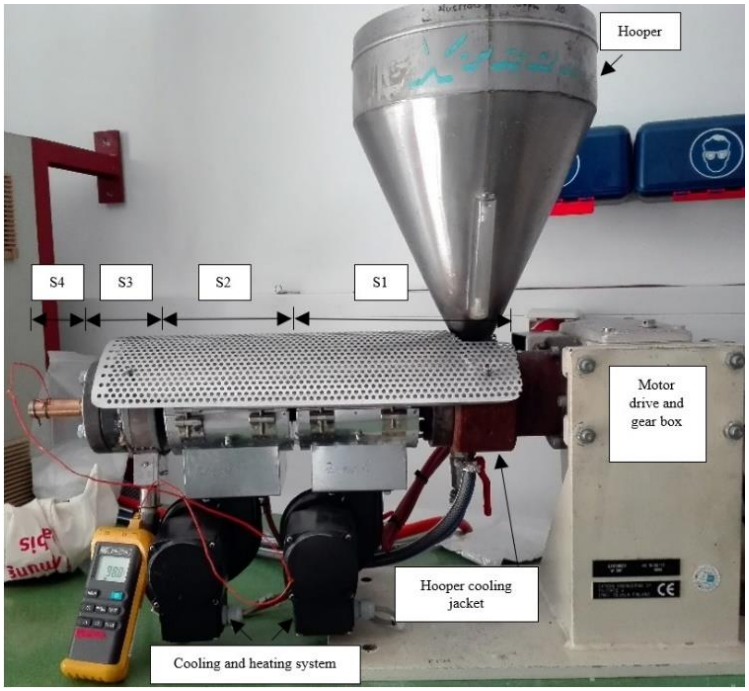

Figure 18: Single screw extruder Extron EX-18-26-1.5

3.2 Methods

Two different thermal analysis were performed to specify the thermal properties of the used resins and CBA's. Additional rheological measurements were conducted to analyse the rheological behaviour of the used thermoplastics. This chapter also defines the methods that were used for the characterization of the foam morphology.

3.2.1 Thermal Analysis

3.2.1.1 Differential scanning calorimetry

Differential scanning calorimetry (DSC) measures the enthalpy and the specific heat capacity as a function of temperature to obtain the melting and crystallisation behaviour. DSC measurements were performed in this thesis to evaluate the thermal properties of the thermoplastic resins and chemical blowing agents, that are not given in the datasheets. A TA

Q2000 DSC was used for the experiments. The measurements were based on the European standards for differential scanning calorimetry for plastics. DIN EN ISO 11357-1:2016 [49] was used for general principles and the determination of temperature of melting and crystallisation were based on ISO/DIS 11357-3:2017 [50]. 5 mg of the sample were put in a standard aluminium pan and heated up with 10 K/min, cooled down and heated up again with the same heating rate. Universal analysis software was used to analyse the data.

3.2.1.2 Thermogravimetric analysis

In addition to the DSC measurements, a thermogravimetric analysis (TGA) was performed. The TGA is a method which measures the mass of a sample as a function of temperature as the sample is subjected to a temperature program. The measurements were based on DIN EN ISO 11358-1:2014 [51], which specifies the general principles for thermogravimetry of polymers. 10 mg of the sample were put in a pan and heated up in a furnace. The mass of the sample is monitored during the experiment. The data was analysed with a universal analysis software.

3.2.2 Rheological measurments

3.2.2.1 Shear viscosity

The discs for the dynamic rheology measurements were compression moulded at 200°C with a heating rate of 15 K/min. They were measured with a plate-plate Anton Paar MCR 301 rheometer under nitrogen with a 1mm gap size. The temperature was set to 180°C with a deformation of 1% and a frequency range from 628 to 0.01 rad/s.

3.2.2.2 Extensional viscosity

For the extensional viscosity measurements sample sheets were compression moulded at 200°C. Rectangular strips with 8 mm width and 15 mm length were cut out of sheets. The experiments were carried out using a Sentmanat Extensional Rheometer for Anton Paar rheometers. Three different strain rates (10 s^{-1}, 1 s^{-1}, 0.1 s^{-1}) were measured at 180°C.

3.2.3 Determination of compressive properties

The compressive strength measurements were based on DIN EN ISO 844 [52], which specifies the methodology of the determination of compressive properties for rigid cellular plastics.

The compression test was performed with a universal testing machine by Zwick Roell. The samples were put between two parallel plates, that were then pushed together. The applied load is distributed across the entire surface area of opposite faces of the sample.

The dimensions and number of samples for the compression test is not conforming to standards as cylindrical samples were produced with a length of 1.5 times the diameter. For the polyethylene and long-chain-branched polypropylene foams a total of five samples were measured, which is in accord with the standard methodology. Only three samples of each polystyrene foam were tested.

A maximum compressive strength below a deformation of 10% is referred to as compressive yield strength σ_{dB}. For those materials that showed a continuing increase of deformation a compressive yield strength could not be determined. The compressive strength at 10% deformation was measured instead. All measurements were performed until a deformation of 50% was reached.

3.2.4 Density determination

The density of the samples was measured by using Archimedes principle. Archimedes principle is based on water displacement.

Distilled water was filled in a beaker and a tensid was added to increase the surface tension. First the weight of the sample in air $W(a)$ is measured, then the sample is submerged in water. The water temperature was also noted. The density of the water was subsequently obtained from literature. The density of the sample was calculated by Eq. 3-1:

$$\rho = \frac{W(a) * [\rho_w - 0.0012]}{0.9983 * G} + 0.0012$$

Eq. 3-1

ρ	density of the sample [g/cm^3]
$W(a)$	weight of the sample in air [g]
ρ_w	density of water [g/cm^3]
G	buoyancy [g]

The average density was obtained by three samples for each processed foam.

3.2.5 Volume expansion ratio

The volume expansion ratio was calculated from the density of the foam and the density of the unexpanded polymer resin [8].

$$V_a = \frac{\rho_p}{\rho_f}$$

Eq. 3-2

ρ_f	foam density [g/cm^3]
ρ_p	density of the unexpanded polymer [g/cm^3]
V_a	volume expansion ratio [−]

3.2.6 Cell density

Three samples transversely to the extrusion direction were obtained for each foam. Then three micrographs of each sample were taken and analysed. In total nine measurements of the cell density were performed for each foam process. The mean value of these nine measurements was calculated, as well as the range and the coefficient of variation.

A quantitative image analysis software was used to measure the average cell size and count the number of cells. It was necessary to increase the contrast between the cells and the polymer matrix. Depending on the cell density either the cells or the cell walls were coloured black. At high cell densities the cell walls were rather thin, thus it was more effective to blacken the cells than the thin cell walls. The number of cells in the analysed area A in the micrograph was determined to calculate the cell density [53].

$$N_0 = \left(\frac{n * M}{A}\right)^{\frac{3}{2}} * \left[\frac{1}{1 - V_f}\right]$$

Eq. 3-3

N_0 cell density [m^{-3}]
n number of cells in A [−]
A area [m^2]
M magnification of the microscope [−]
V_f void fraction [−]

3.2.7 Cell size

The cell size was also obtained through the image analysis software. The cells were first traced in the micrograph and the dimensions of the cells were calculated with the software. The mean cell diameter of all cells in the micrograph was then averaged according to Eq. 3-4 [45].

$$d = \frac{\sum d_i \, n_i}{\sum n_i}$$

Eq. 3-4

d average diameter [m]
d_i diameter of cell i − type [m]
n_i number of cell i − type [−]

3.3 Materials

The experiments were carried out with Hydrocerol as chemical blowing agent and five different thermoplastic resins.

3.3.1 Thermoplastic resins

Five different polymers have been used in the foam extrusion process. Polystyrene is the only amorphous one, the other thermoplastics are semi-crystalline polyethylene and polypropylene resins. The grade names as well as their rheological and thermal data are provided in Table 2:

Table 2: Rheological and thermal properties of the thermoplastic resins

Grade name	MFI [Volume/10min]	Density [g/cm^3]	Glass transition temperature T_g [°C]	Melting temperature T_m [°C]
PS GP 152	2.6*	1.04	91*/91.73	-
PE 290E	-	0.9257	-	112.83
PP HC 600TF	2.8*	0.9127	-	164*
PPWB135 HMS	2.4*	0.8866	-	163*
PPWB140 HMS	2.1*	0.9317	-	163*

*provided in the product data sheet

3.3.1.1 Shear rheology

Additional measurements have been conducted to specify the rheological properties of the used thermoplastics. Figure 19 and Figure 20 give the complex viscosity as well as the storage and loss modulus of the used polymer resins.

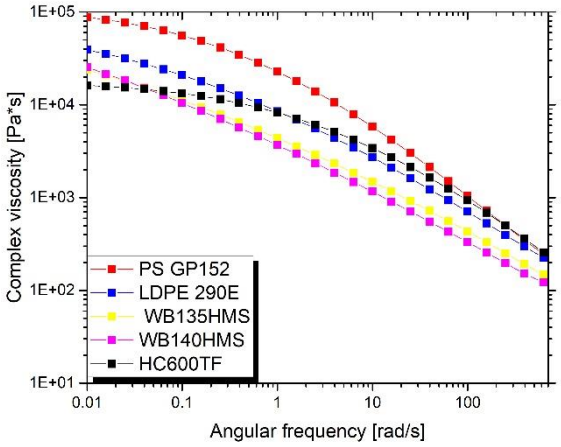

Figure 19: Complex viscosity as a function of the angular frequency of the used thermoplastics at 180°C

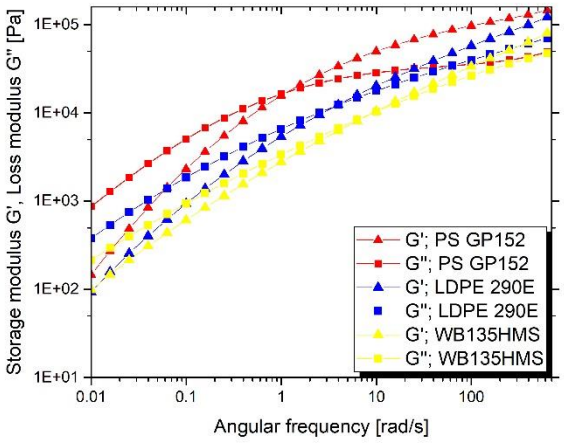

Figure 20: Comparison of the storage and loss modulus of polystyrene, polyethylene and LCB-polypropylene at 180°C

The storage modulus reaches a plateau at higher angular frequencies. A higher plateau modulus can be interpreted as a higher number of molecular alignments of long polymer chains. Those polymers also have a higher molecular weight [42].The plateau is already indicated for some polymers polystyrene (Figure 20) and linear polypropylene (Figure 21). The LCB-PP will reach the plateau modulus at higher angular frequencies. To compare the modulus a reference value at 628 rad/s was determined. Polypropylene HC600TF and polystyrene PS GP152 have the highest modulus.

Table 3: Rheological properties of the thermoplastic resins

Polymer	Modulus G_P at ω=628 rad/s [Pa]	Viscosity η at ω=0.01rad/s
Polypropylene HC600TF	$1.47*10^5$	$1.62*10^4$
Polystyrene PS GP152	$1.46*10^5$	$8.80*10^4$
Polyethylene PE 290E	$1.22*10^5$	$3.91*10^4$
Polypropylene WB135HMS	$8.00*10^4$	$2.38*10^4$
Polypropylene WB140HMS	$6.52*10^4$	$2.55*10^4$

Figure 21 compares storage and loss modulus of linear polypropylene with those of two long chain branched polypropylenes. The viscosity η at ω=0.01rad/s is higher for WB140HMS than for WB135HMS, this indicates a higher molar weight of the polypropylene WB140HMS. The molecular weight of the LCB-PP are significantly higher than that of the linear polypropylene HC600TF.

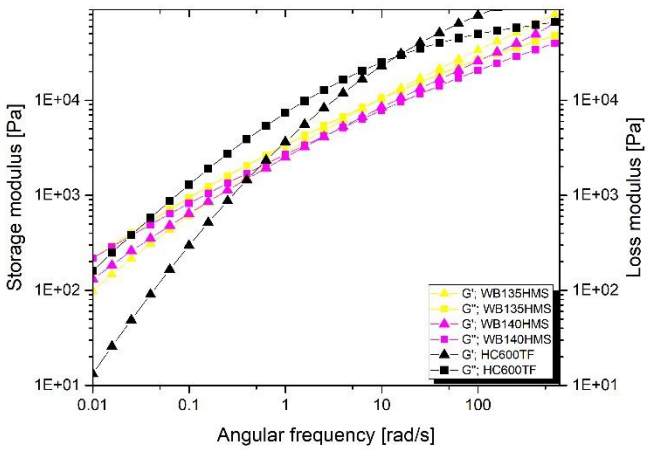

Figure 21: Comparison of the storage and loss modulus of linear polypropylene and LCB-polypropylene at 180°C

The long chain branched polypropylene resins WB135HMS and WB140HMS have the shallowest slopes due to their broad molecular weight distribution (MWD). The MWD of WB140HMS is broader than that of WB135HMS. The linear polypropylene HC600TF has a steeper slope, which indicates a narrower molecular weight distribution compared to those of the LCB-PP.

Linear molecules without any side chains, like HC600TF have a quite narrow molecular weight distribution. The detailed results of the shear viscosity measurements for each resin can be found in the Appendix.

3.3.1.2 Extensional rheology

A comparison of the extensional viscosity as a function of time between linear PP and LCB- PP has been given in Chapter 2.4.2. The two LCB-PP resins (WB135HMS and WB140HMS) exhibit a pronounced strain hardening and quite a similar rheological behaviour as can be seen in Figure 22.

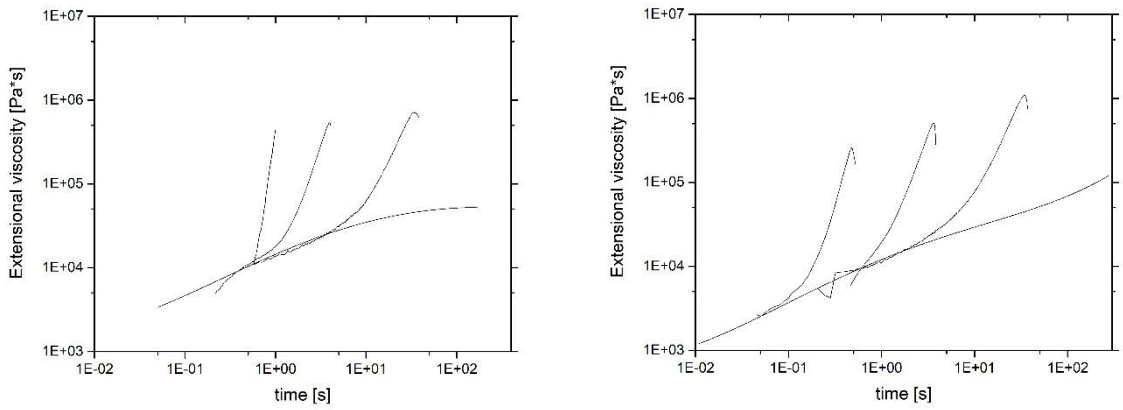

Figure 22: Extensional viscosity of the two LCB-PP resins: WB135HMS (left) and WB140HMS (right) (ε = 10 s^{-1}, 1 s^{-1}, 0.1 s^{-1})

Typical values of the strain rate at extensional flow during the bubble growth lie in the range of 1 s^{-1} to 5 s^{-1} [3]. The linear polypropylene resin does not show any deviation from the start-up curve. In comparison to low-density polyethylene, in which strain hardening was observed. The extensional viscosity of those resins is given in Figure 23.

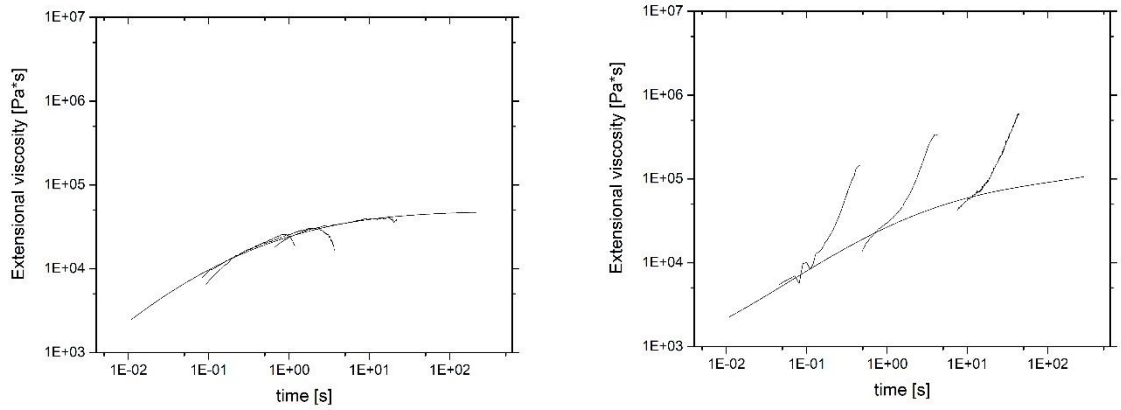

Figure 23: Extensional viscosity of linear PP HC600TF (left) and polyethylene PE 290E (right) (ε = 10 s^{-1}, 1 s^{-1}, 0.1 s^{-1})

As can be seen in Figure 24, polystyrene showed strain hardening only at very high strain rates $\dot{\varepsilon_0} = 10\ s^{-1}$.

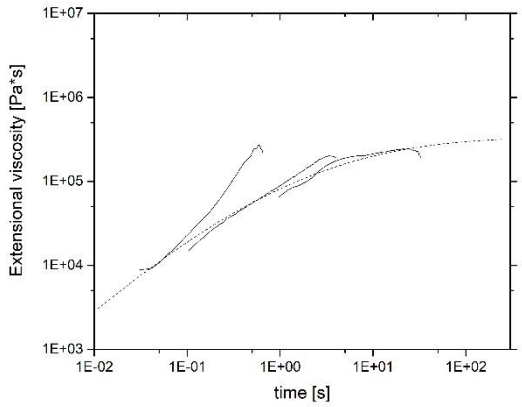

Figure 24: Extensional viscosity of polystyrene PS GP152 (ε = 10 s^{-1}, 1 s^{-1}, 0.1 s^{-1})

The disappearance of the strain hardening behaviour for PS at low strain rates, is commonly noted in literature [3]. The strain hardening of polystyrene comes from $\pi - \pi$ interactions between aromatic rings. Strain hardening has been proofed to be essential for the foamabilty of polyolefins. The role of strain hardening on the foamability has not been clearly defined yet for polystyrene. Explanatory approaches for the good processability take the high degree of plasticization due to the presence of blowing agent and the high energy of activation, that contributes to a rapid solidification and hence cell stabilisation, into account [3].

The strain hardening ratio was calculated to compare the strain hardening of the different polyolefine grades. The strain hardening ratio is defined as the ratio of the maximum extensional viscosity $\eta_{E,max}$ of the rheological melt extension curve and 3 times the extensional viscosity of the frequency sweep curve at the same strain as $\eta_{E,max}$. The strain hardening ratio for the used resins is given in Table 4.

Table 4: Strain hardening ratio SHR

Strain rate $\dot{\varepsilon}$ [s^{-1}]	Strain hardening ratio (SHR) [-]			
	PS GP152	PE 290E	PP WB135HMS	PP WB140HMS
10	5	8	35	32
1	2	11	28	38
0.1	1	7	21	23

The LCB-PP resins WB140HMS and WB135HMS have the highest strain hardening ratio, followed by that of polyethylene PE290E. The strain hardening ratio of polystyrene also shows the disappearance of the strain hardening behaviour for low strain rates.

3.3.2 Chemical blowing agent

Hydrocerol was used as chemical blowing agent. It was supplied by Clariant GmbH. Hydrocerol is a masterbatch consisting of citric acid and sodium bicarbonate. The masterbatches as well as the corresponding carrier material are given in Table 5.

Table 5: Chemical blowing agents

Masterbatch	Carrier material
Hydrocerol PEX 5045	PS
Hydrocerol PEX 5040	PS
Hydrocerol PEX 5024	PE

3.3.2.1 Hydrocerol PEX 5045

Figure 25 shows the results of the differential scanning calorimetry (DSC) of Hydrocerol PEX 5045. The thermogravimetric analysis (TGA) yields consistent results to those of the DSC measurement. Clariant GmbH recommends a minimum processing temperature of 230°C. The results from the DSC and TGA measurement confirms this recommendation (Table 6). The temperature of the feed section can be adjusted to temperatures as high as 140°C, since the decomposition of the masterbatch starts at 190°C. According to information provide by Clariant GmbH Hydrocerol PEX 5045 produces a fine cell structure.

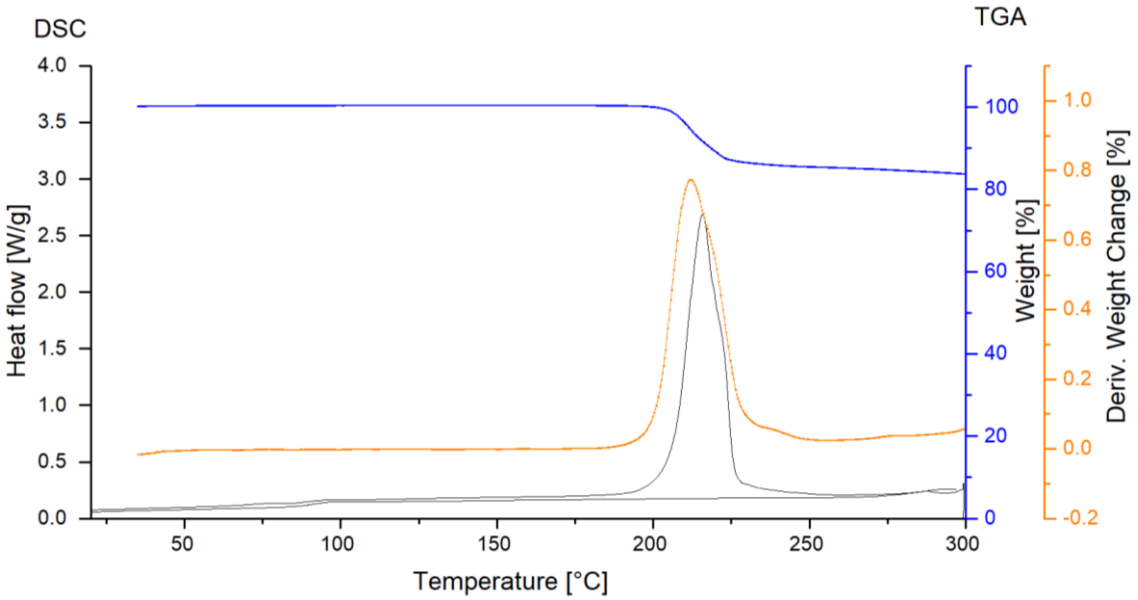

Figure 25: Thermal analysis of Hydrocerol PEX 5045

Table 6: Results of the thermal analysis of Hydrocerol PEX 5045

	DSC results			TGA results		
Peak	T1 [°C]	Tmax[°C]	T2[°C]	T1[°C]	Tmax [°C]	T2 [°C]
1	199	216	229	194	212	230

The TGA also measured the amount of active components. 11,4% of the Hydrocerol PEX 5045 sample remained in the pan. The weight change is 13.7% for the first peak and 2.2% for the second peak. The second peak shows the further decomposition of the carbon acid. The total amount of active components measured with the TGA is 27.4%. According to Clariant GmbH the amount of active components is 30%. The obtained results from the TGA are in accordance with the provided information of the manufacturer.

3.3.2.2 Hydrocerol PEX 5040

According to Clariant GmbH Hydrocerol PEX 5040 has an amount of active components of 40% and provides a high gas yield. Figure 26 shows the five peaks of the measured DSC curve.

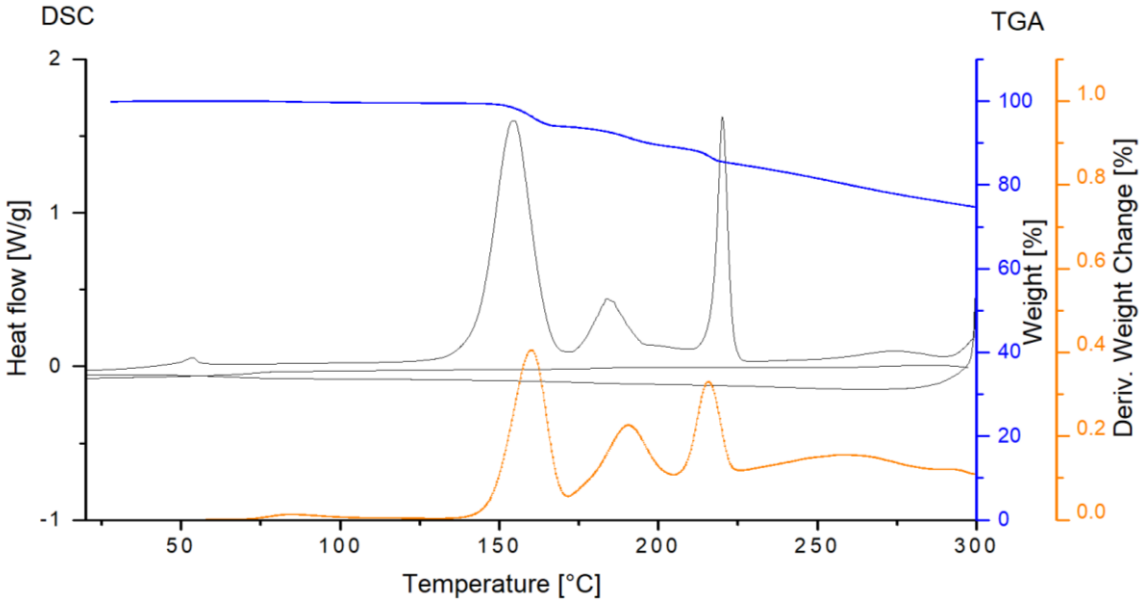

Figure 26: Thermal analysis of Hydrocerol PEX 5040

The decomposition of the citric acid has its maximum at a temperature of 154°C. At 276°C the citric acid decomposes further. The decomposition of the active components has a temperature range from 144°C to 226°C. The TGA measurement also showed five peaks. The peak of the decomposition of the citric acid lies at a temperature of 160°C. The results of the thermal analysis are given in Table 7.

Table 7: Results of the thermal analysis of Hydrocerol PEX 5040

	DSC results			TGA results		
	T1 [°C]	Tmax [°C]	T2 [°C]	T1[°C]	Tmax [°C]	T2 [°C]
1	47	53	57			
2	144	154	169	143	160	173
3	173	184	194	173	190	206
4	210	219	226	206	216	225
5	260	276	290	225	26	300
6				300	313	340

The amount of active components was also determined with the TGA. 15.4% of the sample remained in the pan of the TGA. The weight change is 4.8% for the first peak, 4.7% for the second peak and 3.6% for the third peak. In total, an amount of 28.4% was obtained from the TGA.

3.3.2.3 Hydrocerol PEX 5024

The masterbatch Hydrocerol PEX 5024 has already been used in previous studies on PP foams. The data of the thermal analysis of Hydrocerol PEX 5024 was provided by DI Zoppoth [54]. Figure 27 shows the thermal analysis of the chemical blowing agent.

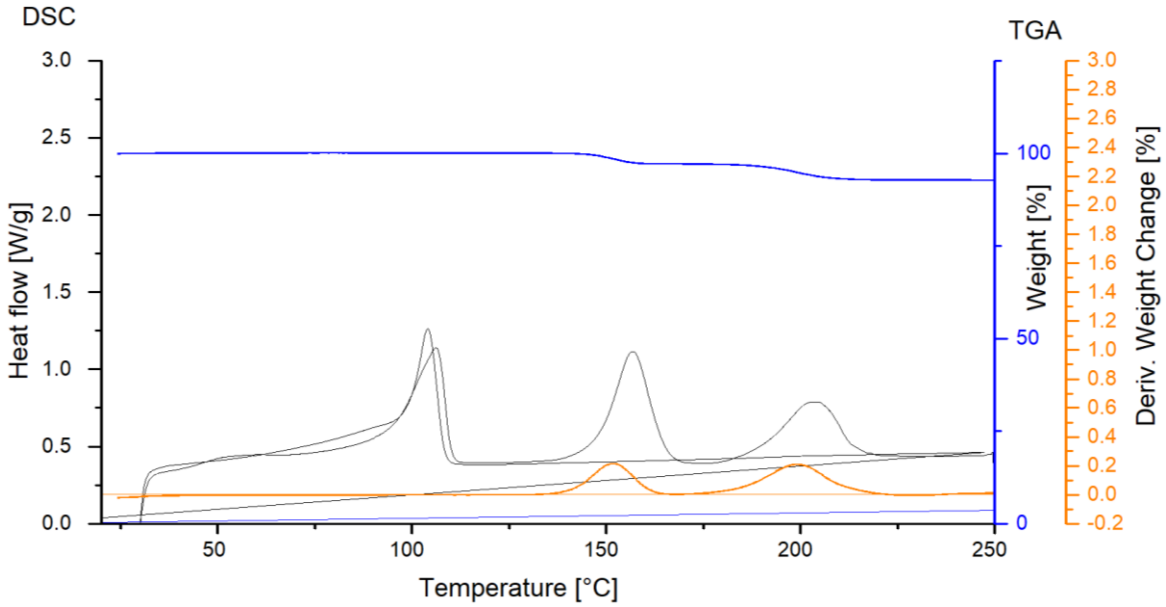

Figure 27: Thermal analysis of Hydrocerol PEX 5024

The optimal processing temperature according to Clariant GmbH is 220°C. The thermal analysis showed that the decomposition is completed at a temperature of 213°C. Peak 3 in Table 8 gives the melting point of the carrier material.

Table 8: Results of the thermal analysis of Hydrocerol PEX 5024

	DSC results			TGA results
Peak	T1 [°C]	Tmax [°C]	T2 [°C]	Tmax [°C]
1	147	157	165	152
2	188	204	214	199
3		105		

3.4 Descriptive statistics

3.4.1 Arithmetic mean and standard deviation

The arithmetic mean $\bar{x}$ and the standard deviation s can be calculated by using Eq. 3-5 or. Eq. 3-6 [55].

Arithmetic mean:

$$\bar{x} = \frac{1}{n}\sum_{i=1}^{n} x_i$$

$\bar{x}$ = arithmetic mean
n = total sample number
x_i = measured values

Standard deviation:

$$s = \sqrt{\frac{1}{n-1}\sum_{i=1}^{n}(x_i - \bar{x})^2}$$

s = standard deviation
$\bar{x}$ = arithmetic mean
n = total sample number
x_i = measured values

Eq. 3-5 or. Eq. 3-6

3.4.2 Range

The range R is a scattering parameter and is the difference between the maximum and the minimum value of a set of data [55].

$$R = x_{max} - x_{min}$$

Eq. 3-7

R= range
x_{max} = maximum value
x_{min} = minimum value

3.4.3 Coefficient of variation

The coefficient of variation v is a relative scattering parameter and is calculated from the ratio of the standard deviation and the arithmetic mean. High values of the arithmetic mean often call forth high values of the variance and standard deviation. The coefficient of variation standardizes the variance and makes the comparison of results easier [55].

$$v = \frac{s}{\bar{x}}$$

Eq. 3-8

v = coefficient of variation
s = standard deviation
$\bar{x}$ = arithmetic mean

3.4.4 Covariance and correlation coefficient

The covariance $Cov(X,Y)$ measures the correlation between two variables. It is calculated by using the Eq. 3-9 [55]:

$$Cov(X,Y) = \frac{1}{n-1}\sum_{i=1}^{n}(x_i - \bar{x}) * (y_i - \bar{y})$$

Eq. 3-9

$Cov(X,Y)$= covariance
$\bar{x}$ = arithmetic mean of the x- component of the sample
n = total sample number
x_i = measured values of the x-component of the sample
$\bar{y}$ = arithmetic mean of the y-component of the sample
y_i = measured values of the y-component of the sample

The correlation coefficient determines the degree of a linear correlation between two variables X and Y. It has a value between -1 and 1. Correlations according to amount of 1 show a tendency of the variables to lie on a line. R = 0 is no linear correlation [55].

$$r = \frac{Cov(X,Y)}{s_x * s_y}$$

Eq. 3-10

r = Correlation coefficient
$Cov(X,Y)$= Covariance
s_x= standard deviation of the x- component of the sample
s_y = standard deviation of the y-component of the sample

4 Single screw extrusion foaming

4.1 Extrusion foaming of polystyrene

Two series of experiments have been conducted to determine the optimal processing parameters for polystyrene foams. The first one was carried out with Hydrocerol PEX 5040, the second one with Hydrocerol PEX 5045.

4.1.1 Hydrocerol PEX 5040

The results of the thermal analysis showed that the start of activation lies at 160°C. Consequently, the temperature in the feed section was set to 130°C. The temperature in the melting section (T2) was set to 235°C. Two additional experiments were performed with T2 = 225°C and T2 = 250°C to evaluate the effect of the melt temperature in Section 2 on the produced foam. The temperature in section 3, as well as the die temperature (T4) were varied. The experiments were performed at three different screw speeds: 25, 40 and 50 rpm. Table 9 shows the conducted experiments in detail.

Table 9: Processing conditions of the extrusion foaming with Hydrocerol PEX 5040 (oD=without section 4)

Sample Nr.	Feed temperature T1[°C]	Melting temperature T2 [°C]	Temperature in section 3 T3 [°C]	Die temperature T4 [°C]	ΔT =(T3-T4) [°C]	Screw speed n [rpm]
PS1A	130.2	235.3	167.0	125.1	41.9	27
PS2A	129.8	235.8	166.2	129.5	36.7	27
PS3A	130.2	235.7	167.0	131.3	35.7	27.5
PS4A	130.0	235.5	165.1	124.9	40.2	49
PS5A	129.9	234.2	162.0	137.2	24.8	27
PS6A	130.5	235.6	165.6	139.6	25.9	38
PS7A	130.2	233.7	163.4	135.6	27.8	50
PS8A	131.0	236.0	170.0	145.0	25.0	27
PS9A	130.5	235.3	171.1	148.0	23.1	49
PS10A	130.0	233.0	170.0	146.0	24.0	40
PS11A	129.6	235.3	181.3	151.5	29.8	27
PS12A	129.9	235.0	177.2	139.6	37.6	27
PS13A	130.0	224.9	167.8	136.2	31.6	27
PS14A	129.6	251.5	166.5	131.4	35.1	27
PS15A	129.6	235.0	162.2	oD	-	27
PS16A	129.6	235.0	162.2	oD	-	50

4.1.2 Hydrocerol PEX 5045

Since the decomposition of this masterbatch starts at 200°C, the feed temperature could be lifted to 140°C. The melting section temperature was set to 235°C and additional experiments at 250°C were conducted as well. The variation of the die temperature T4, the temperature T3 and

the screw speed were performed analogous to 4.1.1. The set parameters for the foam processes are listed in Table 10.

Table 10: Processing conditions of the extrusion foaming with Hydrocerol PEX 5045 (oD=without section 4)

Sample Nr.	Feed temperature T1 [°C]	Melting temperature T2 [°C]	Temperature in section 3 T3 [°C]	Die temperature T4 [°C]	ΔT =(T3-T4) [°C]	Screw speed n [rpm]
PS1B	140.4	235.2	167.0	124.5	42.5	27
PS2B	139.3	236.7	160.7	123.8	36.9	50
PS3B	140.0	235.7	161.5	133.2	28.3	26.5
PS4B	140.4	235.3	161.5	134.5	27.0	49
PS5B	139.3	235.7	170.9	146.3	24.6	27
PS6B	140.0	235.0	170.0	146.4	23.6	50
PS7B	140.0	236.1	171.1	143.0	28.1	40
PS8B	139.9	233.4	181.3	156.1	25.3	26.5
PS9B	139.9	235.0	176.1	143.7	32.4	26
PS10B	140.1	247.3	179.7	142.7	37.0	27
PS11B	140.1	250.0	189.3	147.6	41.7	27
PS12B	139.3	236.7	163.4	oD	oD	27
PS13B	139.3	236.7	163.4	oD	oD	50

4.2 Results of the extrusion foaming of polystyrene

4.2.1 Effect of set parameters

4.2.1.1 Hydrocerol PEX 5040

According to the information provided by Clariant GmbH a high gas yield can be achieved with the masterbatch Hydrocerol PEX 5040. This led to the formation of big gas bubbles and cell coalescence (Figure 28). The cell coalescence tends to be less pronounced with lower die temperature T4. The temperature difference between T3 and T4 is a crucial criterion for a good

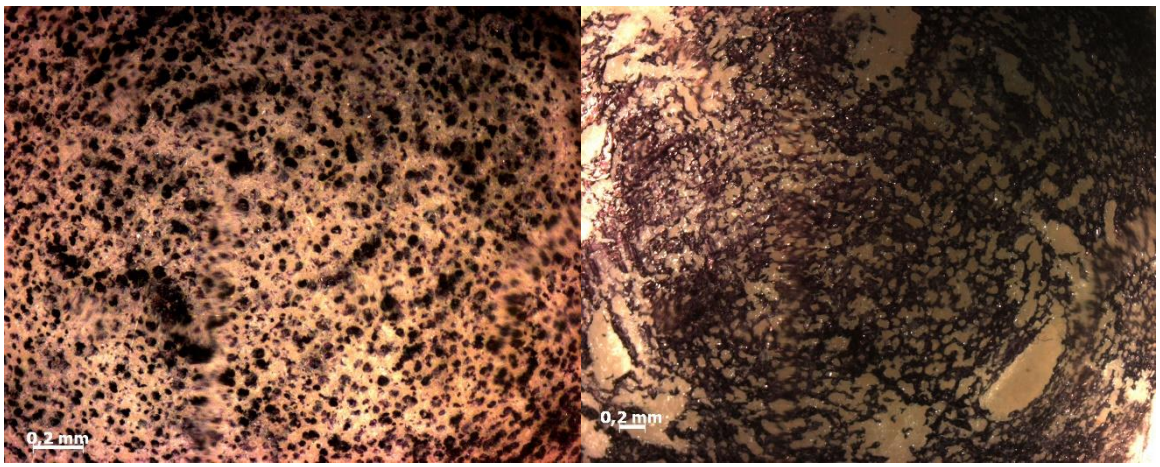

Figure 28: left: sample PS2A, fine cells at the centre; right: sample PS12A: cell coalescence and big gas bubbles

foam quality. The higher the temperature difference, the finer and more homogenic bubbles were produced.

The difference of the die temperature of the samples PS2A (T4 = 129.5°C) and PS12A (T4 = 139.6°C) is 10.1°C. In sample PS12A the cell coalescence is quite pronounced over the whole cross-section. In the sample PS2A cell coalescence can only be found at the outer region of the cross-section. This can be seen in Figure 28. The cell coalescence at the outer region of the sample is produced by higher shear stress, which is caused by the die (Chapter 2.6).

The screw speed also has an influence on the quality of the produced foams. High screw speeds (40, 50 rpm) promote the formation of larger gas bubbles. In principle it can be stated, that the quality of the foam is better, the lower T4 and the higher the temperature difference ΔT is. Consequently, experiments with a die temperature above 135°C, a temperature difference below 35°C and high screw speeds will not be discussed in detail.

The experiments also showed that a higher temperature in the melting section did not improve the quality of the foam. The experiments without the additional die section (T4) had high cell coalescence. It was not as pronounced in the sample PS15A as in PS16A, but both had a lower foam quality than the experiments with the additional section 4.

4.2.1.2 Hydrocerol PEX 5045

As mentioned previously, the masterbatch Hydrocerol PEX 5045 produces a fine cell structure. The produced foams tend to be less susceptible to cell coalescence than those produced with Hydrocerol PEX 5040. A high screw speed (40, 50 rpm) promotes cell coalescence, which is in accord with the results of foams produced with Hydrocerol PEX 5040. This can be seen in Figure 29.

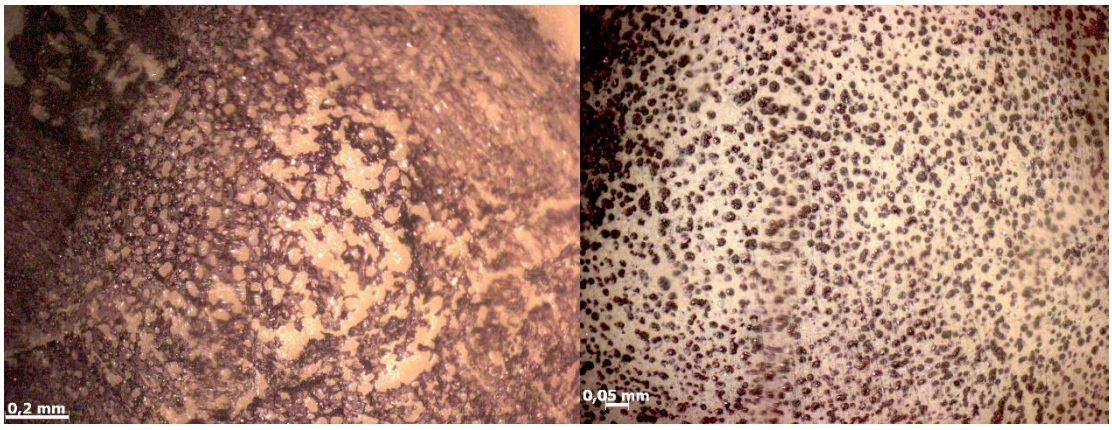

Figure 29: left: sample PS6B shows cell coalescence (50 rpm); right: sample PS9B no cell coalescence

It could be confirmed for this batch as well, that the die temperature T4 has a significant effect on the quality of the produced foam. A too high die temperature, as seen in sample PS11B, leads to cell coalescence and the formation of big gas bubbles. It is not necessary to keep the die temperature as low as 125°C, like with Hydrocerol PEX 5040. As can be seen in Figure 30,

a die temperature of 143.65°C (sample PS9B) produces a good foam quality without cell coalescence or big gas bubbles.

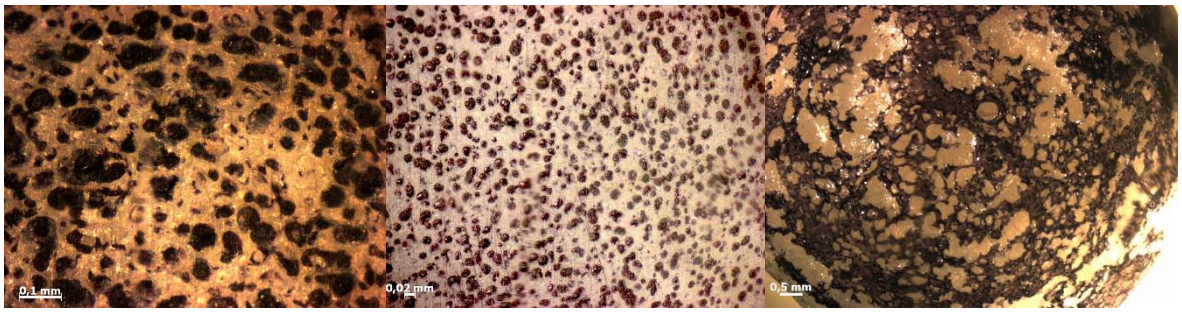

Figure 30: Micrographs of polystyrene foams; left: sample PS1B (T4=124.45°C); middle: sample PS9B (T4=143.65°C), right: sample PS11B (T4=147.6°C)

The experiments with Hydrocerol PEX 5045 and a high temperature in the melting section (T2) also did not show a significant improve of the produced foam. Noticeable is the result without the additional die (T4). The sample PS12B had despite the high die temperature (163.4°C) a fine cell structure without the formation of big gas bubbles.

4.2.2 Foam morphology

In order to examine the quality of the produced foams the mean cell density as well as the mean cell size were determined. Table 11 only lists the results of the best foam samples. All foams that are not noted in Table 11 either did not have a homogeneous foam morphology due to the formation of large gas bubbles or were unfoamed.

Table 11: Mean cell density and mean cell diameter of the polystyrene foams

Nr.	Mean cell density [cm^{-3}]	Variation coefficient [%]	Range R [cm^{-3}]	Mean cell diameter $\bar{d}$ [mm]	Standard deviation of the mean cell diameter [mm]
PS1A	$5.17*10^8$	20.26	$2.93*10^8$	0.022	0.01
PS2A	$5.80*10^8$	43.73	$6.76*10^8$	0.028	0.02
PS3A	$1.98*10^8$	39.71	$2.66*10^8$	0.039	0.02
PS13A	$3.23*10^8$	34.88	$4.58*10^8$	0.033	0.02
PS14A	$5.66*10^7$	13.49	$2.40*10^7$	0.034	0.01
PS9B	$4.18*10^8$	34.57	$5.69*10^8$	0.027	0.01
PS10B	$7.36*10^7$	35.90	$9.12*10^7$	0.045	0.03
PS12B	$3.02*10^8$	39.23	$3.82*10^8$	0.027	0.01

A microcellular foam has a cell density in the range of 10^9 cm^{-3} and 10^{15} cm^{-3} [56]. The produced cell density is in the range of 10^7 cm^{-3} and 10^8 cm^{-3}, which is at the lower boundary of a microcellular foam. The sample PS2A had the highest cell density of the foams produced with Hydrocerol PEX 5040. For the ones with Hydrocerol PEX 5045 it was sample PS9B.

The variation coefficient of the cell density varies between 13.49% and 43.73%. Hence, the measured cell density underlies enormous fluctuations even though three samples over the length of the foam strand had been taken. This implies that the cell density changes over the

length of the foam. This prompts that the measured values of the cell density cover a large range. Since the experiments indicated that the die temperature influences the foam quality, this correlation was evaluated with a scatterplot (Figure 31).

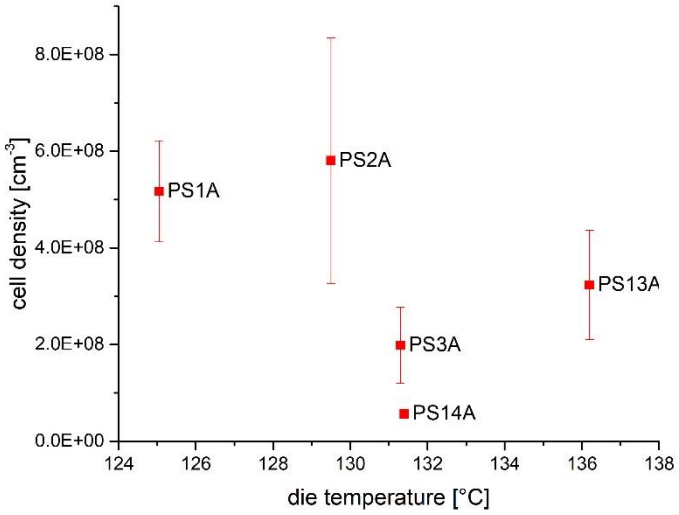

Figure 31: Mean cell density as a function of the die temperature

Figure 31 does not show a direct correlation between the cell density and the die temperature at first glance. In this connection, the high variation coefficient must be considered as well. In Figure 31 the standard deviation is plotted as error indication.

During the foam process the temperature in section 3 and 4 was subject to fluctuations as well. In some cases, the temperature increased up to 3°C. The temperature at the die was measured at the beginning and at the end of each experiment. The resulting mean values are listed in 4.1.1 and 4.1.2. The scattering plot (Figure 32) shows the correlation between the variation coefficient of the cell density and the die temperature.

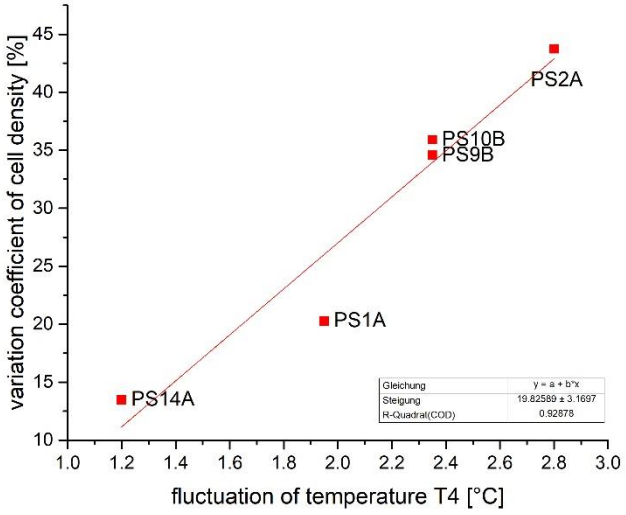

Figure 32: Linear correlation of the temperature and cell density fluctuation

The RSQ of the straight line is 0.9288. This leads to the assumption of a linear correlation between these two variables. The covariance and the correlation coefficient were calculated to testify this. The latter must have a value according to 1 to show a linear correlation.

Table 12: Correlation of the fluctuation of the cell density and the fluctuation of the die temperature

Covariance	5.71
Correlation coefficient	0.96

The results in Table 12 confirm the correlation of the variation coefficient of the cell density and the fluctuation of the die temperature. A correlation between the cell density and the die temperature can therefore be assumed. Due to the high fluctuations of the die temperature it is not possible to assign the measured cell densities to a defined temperature. Thus, a correlation between the cell density and the die temperature cannot be measured directly.

Even though the numeric values of the mean cell densities underlie high insecurities, the order of the magnitude can be used for comparison. Both masterbatches produce foams with a cell density in the range of 10^8. The mean cell diameter is between 0.02 mm and 0.04 mm.

4.2.3 Foam density and compressive strength

Besides the cell density, the foam density was determined as well. The foam density of the best samples lies between 0.320 and 0.392 g/cm^3. The volume expansion coefficient has values between 1.89 and 3.25.

Table 13: Foam density and volume expansion ratio of the polystyrene foams

Sample Nr.	Foam density [g/cm^3]	Standard deviation [g/cm^3]	Volume expansion ratio [-]
PS1A	0.486	0.034	2.14
PS2A	0.320	0.012	3.25
PS3A	0.430	0.133	2.42
PS13A	0.341	0.017	3.05
PS14A	0.550	0.046	1.89
PS9B	0.392	0.066	2.66
PS10B	0.475	0.044	2.19
PS12B	0.533	0.017	1.95

All measured samples of the PS B series (Hydrocerol PEX 5045) and most of the samples of the PS A series (Hydrocerol PEX5040), except PS3A and PS11A showed a significant compressive yield strength. For the samples PS3A and PS11A the compressive strength at 10%

deformation was determined. The obtained values are given in Table 14 and the corresponding compressive strength-deformation plots are provided in Figure 33.

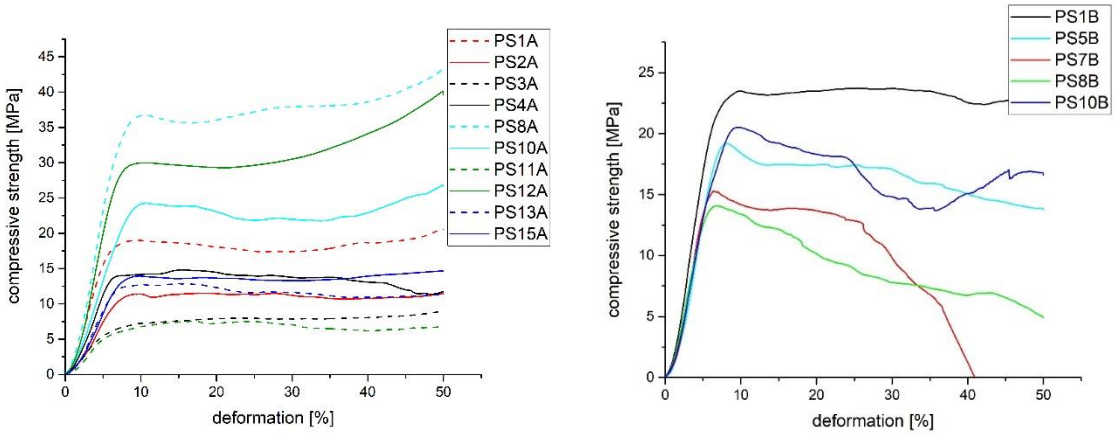

Figure 33: Compressive strength measurements of PS A foams (left) and of PS B foams (right)

Foams produced with Hydrocerol PEX 5040 (PS A series) show a proportional increase in deformation with rising load until a maximum value is reached (compressive yield strength). At the compressive yield strength, the weakest cell walls of the foam begin to break leading to a decrease of compressive strength with further deformation. The measurements were carried out up to a deformation of 50%. As can be seen in Figure 33, the polystyrene foams show plastic deformation, but the overall cell structure of the foams can withstand the compressive loads.

This material behaviour towards compressive load differs from the polystyrene foams produced with Hydrocerol PEX 5045, except for the sample PS1B. Most of the foams produced with Hydrocerol PEX 5045 (PS B series) have shown a continuing decrease of compressive strength after the compressive yield strength is reached.

As can be seen in Figure 33, the compressive yield strength of the PS A foams covers a range from 6.8 MPa to 36.8 MPa. The plotted curves are the mean of the single measurements. Figure 34 shows the mean compressive yield strength and the standard deviation of the compressive strength. It can be seen, that the foams with the highest compressive yield strength, PS8A and PS10A, also have the highest standard deviation. Those foams show an inhomogeneous morphology over the length of the foam strand and consequently a poor foam quality due to the too high die temperature. The foam PS12A had a high compressive yield strength due to the poor foam quality, as can be seen in Figure 28. For this reason, the foam morphology of those samples was not analysed further. Except for the samples PS3A and PS11A the compressive yield strength tends to increase with increasing foam density. The foam sample PS3A has quite a low compressive strength, this is caused by the formation of bigger gas bubbles at the outer regions of the sample. The compressive strength was measured over the whole cross-section of the sample, but the foam density was analysed only at the inner region.

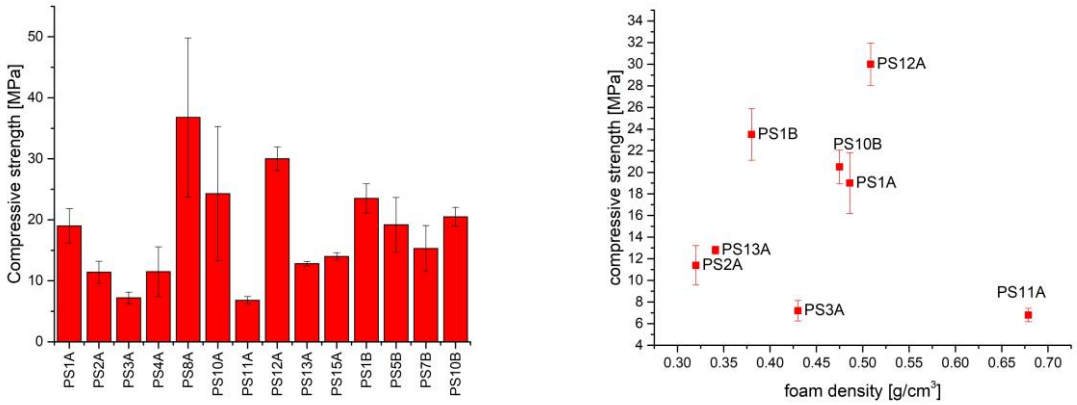

Figure 34: Compressive yield strength of PS A and PS B foams (left) and compressive yield strength as a function of foam density (right)

Table 14 gives the compressive yield strength and the compressive strength at 10% deformation. The compressive yield strength is reached at deformations between 6 to 11%, which is relatively high for a polystyrene foam.

The compressive strength is dependent on the foam density. The volume expansion ratio of the best foam (PS2A) was only 3.25. The compressive yield strength of foams with the best foam qualities are all below 19 MPa.

Table 14: Compressive yield strength σ_{DB} and compressive strength at 10% deformation σ_{D10} of the polystyrene foams

Sample Nr.	σ_{DB} [MPa]	ε_{DB} [%]	σ_{D10} [MPa]	ε_{D10} [%]
PS1A	19.0	9.6		
PS2A	11.4	10.0		
PS3A	-	-	7.2	10.0
PS4A	11.5	10.7		
PS8A	36.8	10.5		
PS10A	24.3	10.8		
PS11A	-	-	6.8	10.0
PS12A	30.0	10.4		
PS13A	12.8	10.1		
PS15A	14.0	9.8		
PS1B	23.5	9.8		
PS5B	19.2	8.2		
PS7B	15.3	6.4		
PS10B	20.5	9.6		

The foam density is also influenced by the formation of bigger gas bubbles, because this decreases the density significantly. This also stands for the compressive yield strength. This can be seen at the foam sample PS4A, which had a quite inhomogeneous cell morphology and bigger gas bubbles throughout the strand. Accordingly, the compressive yield strength of this sample is quite low.

4.2.4 Summary of Polystyrene

Considering the mentioned criteria for a good foam quality, the best polystyrene foam was PS2A, which was foamed with Hydrocerol PEX 5040. The properties of this foam are given in Table 15.

Table 15: Properties of the best polystyrene foam

	PS2A
Masterbatch	PEX 5040
Die temperatureT4 [°C]	129.5
ΔT [°C]	36.7
Screw speed n [rpm]	27
Mean cell density [cm^{-3}]	$5.80*10^{8}$
Mean cell diameter [mm]	0.028
Foam density [g/cm^{3}]	0.320
Volume expansion ratio [-]	3.25
Compressive yield strength [MPa]	11.4

As mentioned above, the die temperature is a critical parameter of the foam process. A high gas yield and the resulting cell coalescence can be controlled with a low die temperature. For a fine cell structure, as it is produced by Hydrocerol PEX 5045, a higher die temperature can be set. The quality of the foam can be improved by the usage of the die temperature section S4. The die section S4 is essential when an accurate temperature control is needed, and a low die temperature is favoured.

Based on the high variation coefficient of the cell density it is shown that even small temperature fluctuations at the die influence the results of the cell density and consequently the quality of the foam.

4.3 Extrusion foaming of low-density polyethylene

The activation of Hydrocerol PEX 5024 starts at 147°C. The temperature in the feed section should be set 5°C above the melting temperature of the resin at the most. The melting point of the low-density polyethylene lies at around 100°C. The temperature in the melting section is chosen depending on the decomposition of the masterbatch. It is completed at 220°C. The temperature in section 3 and the die temperature were varied. The screw speed was set to 27 rpm. Detailed information of the set parameters is given in Table 16.

Table 16: Processing conditions of the extrusion foaming of LDPE

Sample Nr.	Feed temperature T1[°C]	Melting temperature T2 [°C]	Temperature in section 3 T3 [°C]	Die temperature T4 [°C]	ΔT =(T3-T4) [°C]	Screw speed n [rpm]
PE1	110.0	219.8	142.4	114.5	27.9	27
PE2	110.3	221.3	146.8	117.0	29.8	27
PE3	109.9	221.5	165.8	120.6	45.2	27
PE4	109.7	220.2	174.4	125.4	48.9	27
PE5	110.3	218.7	180.3	135.0	45.3	27

The foaming processes were done at temperatures right above the melting point of the LDPE resin. Due to the inefficient cooling in section 3 and 4, the temperature T3 and consequently the die temperature T4 depend on the set temperature in the melting section T2. The temperature T4 could not be lowered without risking an incomplete decomposition. This limited the achieved temperature T4 to 110°C.

4.4 Results and discussion of the extrusion foaming of low-density polyethylene

4.4.1 Effect of set parameters

A correlation between the quality of the foam and the die temperature T4 has already been determined with the produced PS foams. This has also been observed with the LDPE foams.

All samples showed a homogenic cell distribution over the entire cross section. The formation of big gas bubbles did not appear. This can be seen in Figure 35.

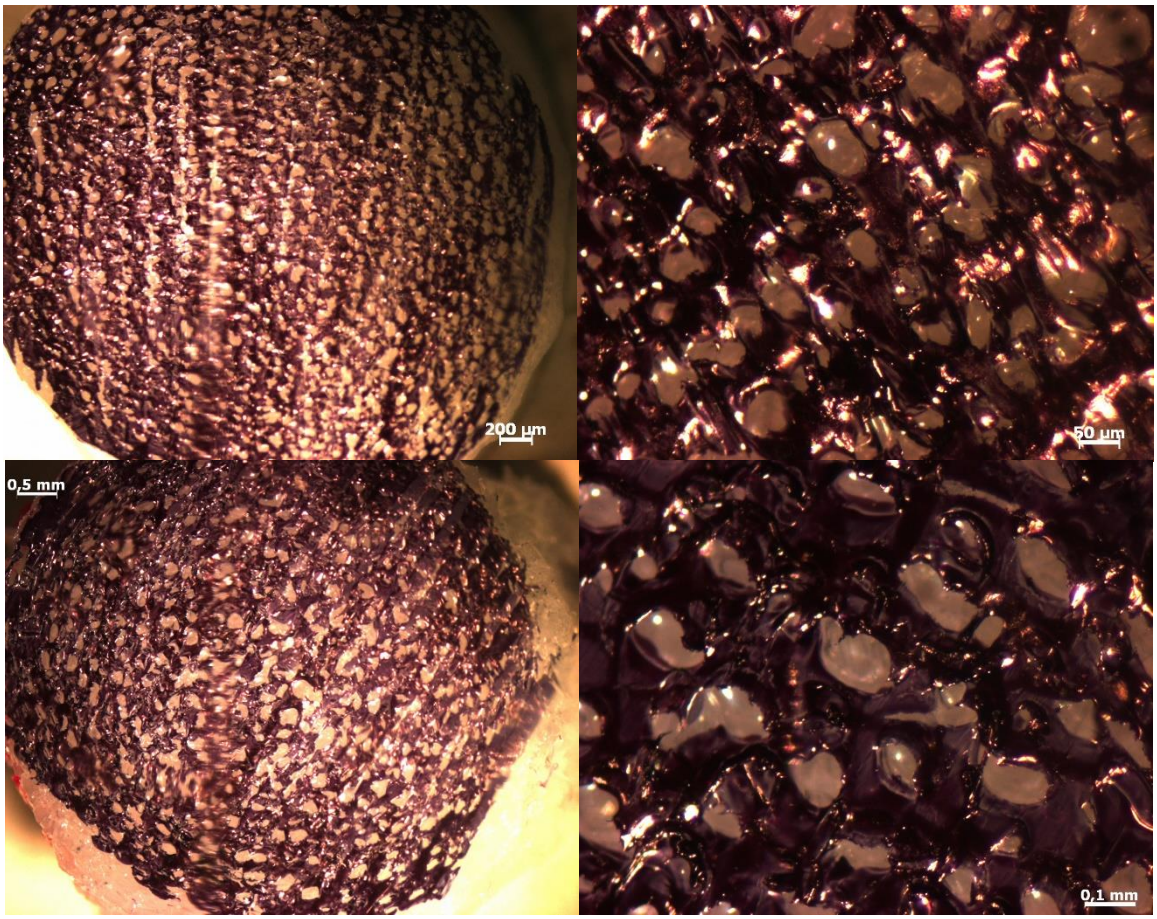

Figure 35: Micrographs of the LDPE foams; top: PE1, bottom: PE5

4.4.2 Foam morphology

The cell density and the cell size were measured to determine the foam quality. The results are given in Table 17.

Table 17: Mean cell density and mean cell diameter of the LDPE foams

Sample Nr.	Mean cell density [cm^{-3}]	Variation coefficient [%]	Range R [cm^{-3}]	Mean cell diameter $\bar{d}$ [mm]	Standard deviation of the mean cell diameter [mm]
PE1	$5.62*10^7$	12.40	$2.13*10^7$	0.038	0.02
PE2	$6.42*10^7$	17.00	$2.95*10^7$	0.039	0.02
PE3	$9.66*10^6$	25.16	$8.36*10^6$	0.056	0.03
PE4	$4.20*10^7$	32.61	$4.07*10^7$	0.041	0.02
PE5	$2.11*10^7$	23.15	$1.43*10^7$	0.047	0.02

The cell density reduces with rising die temperature. The mean cell diameter of the LDPE foams on the contrary rises with rising die temperature. This is visualised in Figure 36. The sample PE3 has a low cell density, which is likely caused due to high temperature fluctuations. Apart

from this sample, the other foams show a linear correlation of the cell density and the die temperature.

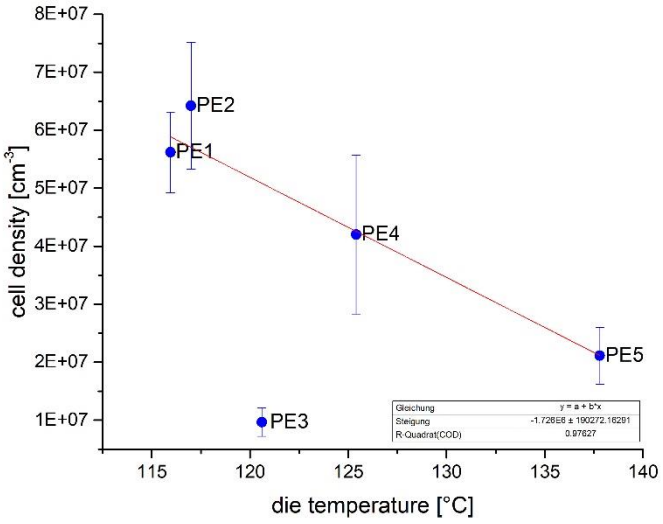

Figure 36: Cell density as a function of the die temperature. Note the significantly higher cell density at lower die temperatures

Figure 37 shows the correlation between the variation coefficient and the fluctuation of the die temperature T4. The variation coefficient and consequently the inhomogeneity of the cell density tends to rise with rising temperature fluctuations. The sample PE5 has a lower variation coefficient than the sample P4, it was not considered in the linear fit shown in Figure 32. PE5 also has a low cell density. This is likely caused by a too high die temperature.

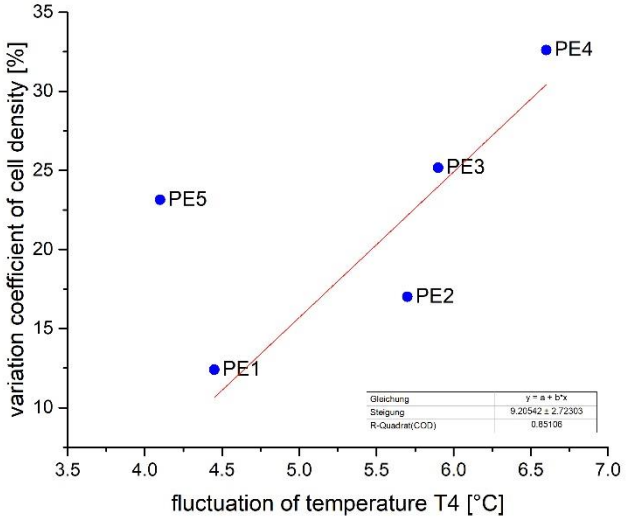

Figure 37: Correlation of the temperature and cell density fluctuation

4.4.3 Foam density and compressive strength

The foam density of the produced LDPE foams lies between 0.500 and 0.578 g/cm^3, as can be seen in Table 18. The lowest density could be achieved with the samples, that were foamed with the lowest die temperatures. The volume expansion ratio has values between 1.60 and 1.83 and is lower than the volume expansion ratio of the polystyrene foams.

Table 18: Foam density and volume expansion ratio of the LDPE foams

Sample Nr.	Foam density [g/cm^3]	Standard deviation [g/cm^3]	Volume expansion ratio [-]
PE1	0.506	0.0159	1.83
PE2	0.533	0.0257	1.74
PE3	0.500	0.0023	1.85
PE4	0.578	0.0020	1.60
PE5	0.552	0.0055	1.68

The material behaviour towards compressive load of polyethylene foams is quite different from that of polystyrene foams. The polyethylene foams did not show a compressive yield strength, but a continuous deformation with increasing load. Thus, the compressive strength at 10% deformation was determined and compared (Table 19). The measured material behaviour under compression load is given in Figure 38.

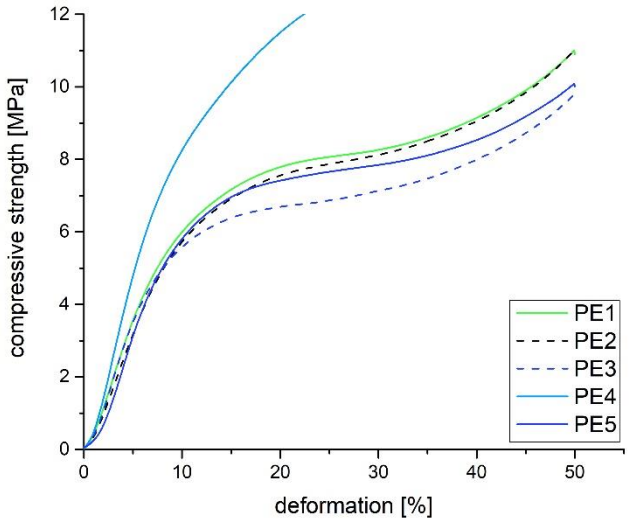

Figure 38: Compressive strength of polyethylene foams

The produced polyethylene foams had the most homogeneous foam morphology of all produced foams. This results in a quite similar material behaviour under compression load, as can be seen in Figure 39.

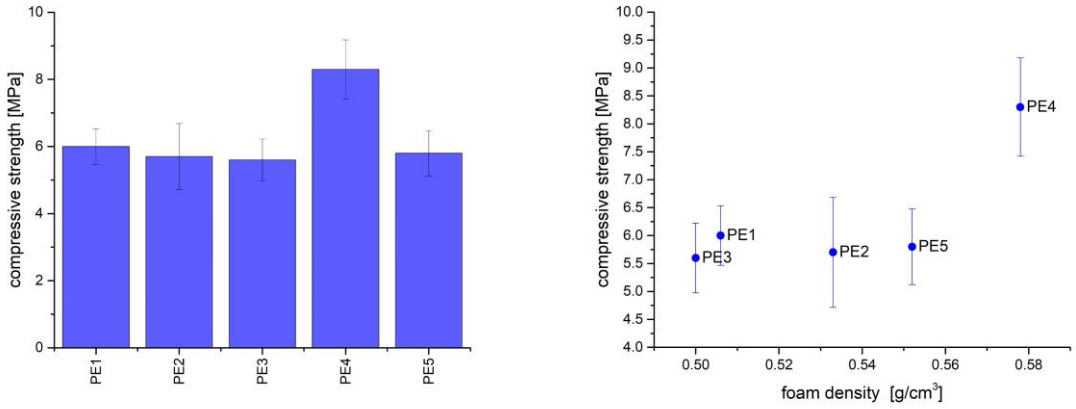

Figure 39: Compressive strength σ_{D10} (left) and compressive strength as a function of foam density (right)

The higher compressive strength of the foam PE4 results from the higher foam density as well as the high variation coefficient of the cell density which indicates an inhomogeneous foam morphology.

Table 19: Compressive strength at 10% deformation of polyethylene foams

Sample Nr.	σ_{D10} [MPa]	ε_{D10} [%]
PE1	6.0	10.0
PE2	5.7	10.0
PE3	5.6	10.0
PE4	8.3	10.0
PE5	5.8	10.0

4.4.4 Summary of low-density Polyethylene

The best result of the extrusion foaming of LDPE is given in Table 20.

Table 20: Properties of the best low-density polyethylene foams

	PE1
Masterbatch	PEX 5024
T4 [°C]	114.45
ΔT [°C]	27.9
Screw speed n [rpm]	27
Mean cell density [cm^{-3}]	$5.62*10^7$
Mean cell diameter [mm]	0.038
Foam density [g/cm^3]	0.506
Volume expansion ratio [-]	1.83
Compressive strength (at ε_{D10}) [MPa]	6.0

In absolute values the cell density of PE1 was only topped by the sample PE2, but the actual values are distorted by the temperature fluctuations. The variation coefficient and the range of the cell density examine this closer. The cell density of the best samples of LDPE foam lies at 10^7 cm^{-3}. The sample PE1 has the lowest mean cell diameter and variation coefficient. The

range of the cell density of PE1 was also one of the lowest. It was not possible to examine, if an additional temperature reduction below 110°C would have improved the foam quality significantly. The temperature control of the die was quite challenging for the LDPE foaming, the fluctuations were as high as 7°C for some samples.

4.5 Extrusion foaming of linear PP and LCB-PP

The foam process of linear PP and LCB-PP were also done with Hydrocerol PEX 5024. The crystallisation temperature of the used LCB-PP was at about 127°C, so the temperature of the feed section was set to 135°C. The detailed information on the set parameters is listed in Table 21.

Table 21: Processing conditions of the extrusion foaming of PP and LCB-PP

Sample Nr.	Feed temperature T1[°C]	Melting temperature T2 [°C]	Temperature in section 3 T3 [°C]	Die temperature T4 [°C]	ΔT =(T3-T4) [°C]	Screw speed n [rpm]
PP1	133.8	221.8	162.2	130.9	31.3	27
PP2	135.2	220.8	174.7	134.1	40.6	27
PP3	134.8	218.9	175.7	136.1	39.6	27
PP4	135.1	220.5	180.1	141.8	38.3	27
WB1	135.2	220.1	173.5	129.6	43.9	27
WB2	135.2	218.9	173.8	133.5	40.3	27
WB3	134.9	220.0	164.8	137.1	27.7	27
WB4	135.2	220.8	195.3	146.0	49.3	27
WBA	134.9	221.3	172.8	130.6	42.2	27
PP#PODIC	130.5	220.8	190.3	136.2	54.5	27

The sample WB1- WB4 were done with the PP135HMS resin, the sample WBA was foamed with PP140HMS.

For the foam PP#PODIC, linear polypropylene HC600TF was long chain branched with peroxydicarbonates (PODIC) by reactive extrusion and foamed with a chemical blowing agent in one step. The polypropylene resin HC600TF and the chemical blowing agent Hydrocerol PEX5024 were shredded with a granulator, mixed with PODIC and fed to the single screw extruder.

4.6 Results and Discussion of the extrusion foaming of PP and LCB-PP

4.6.1 Effect of the set parameter

The die temperature for the foaming of linear PP had to be 10°C higher than the cristallisation temperature. Otherwise the viscosity was to low and the die got blocked. The die temperature had an influence on the quality of the produced foams. At higher die temperatures, as can be seen with the sample PP4, the cell density was relative low. This can also be noticed in the micrographs (Figure 40). It can also be seen that the processing window of linear PP is quite small. The temperature difference between the samples PP1 and PP2 is only 3.15°C, but the sample PP2 already shows cell coalescence at the outer regions.

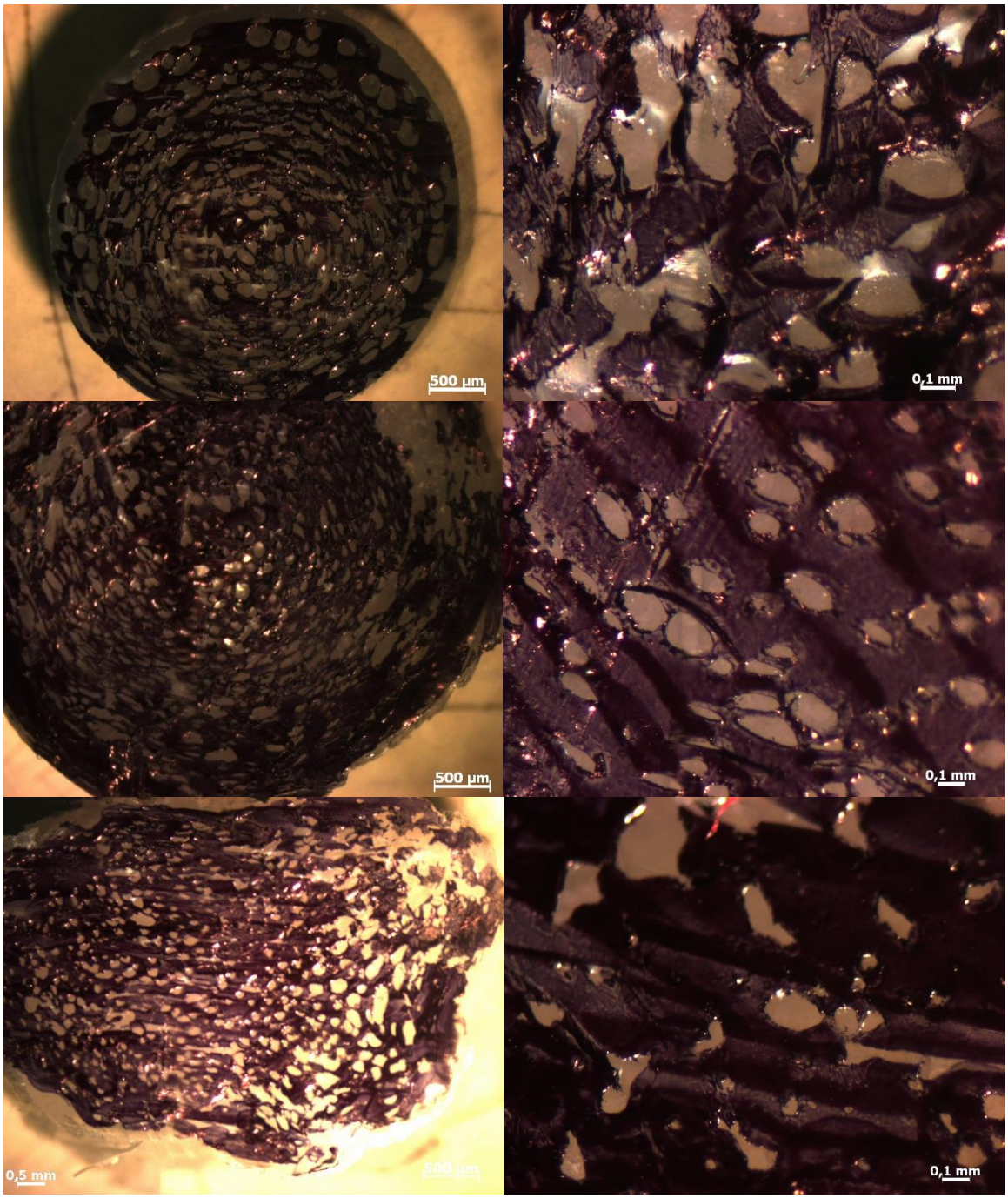

Figure 40: Micrographs of the polypropylene foams; top: PP1, middle: PP2, bottom: PP4

The foaming of LCB-PP was also improved at lower die temperatures. The lowest possible die temperature was limited by the crystallisation temperature of the LCB-PP resin. The samples WB1 and WB2 had compared to the other HMS samples a relatively homogenic cell distribution (Figure 41). The cell distribution got more and more inhomogenic at higher die temperatures (WB3, WB4), promoting the formation of bigger gas bubbles and cell coalescence. This is also apparent at the higher mean cell diameter.

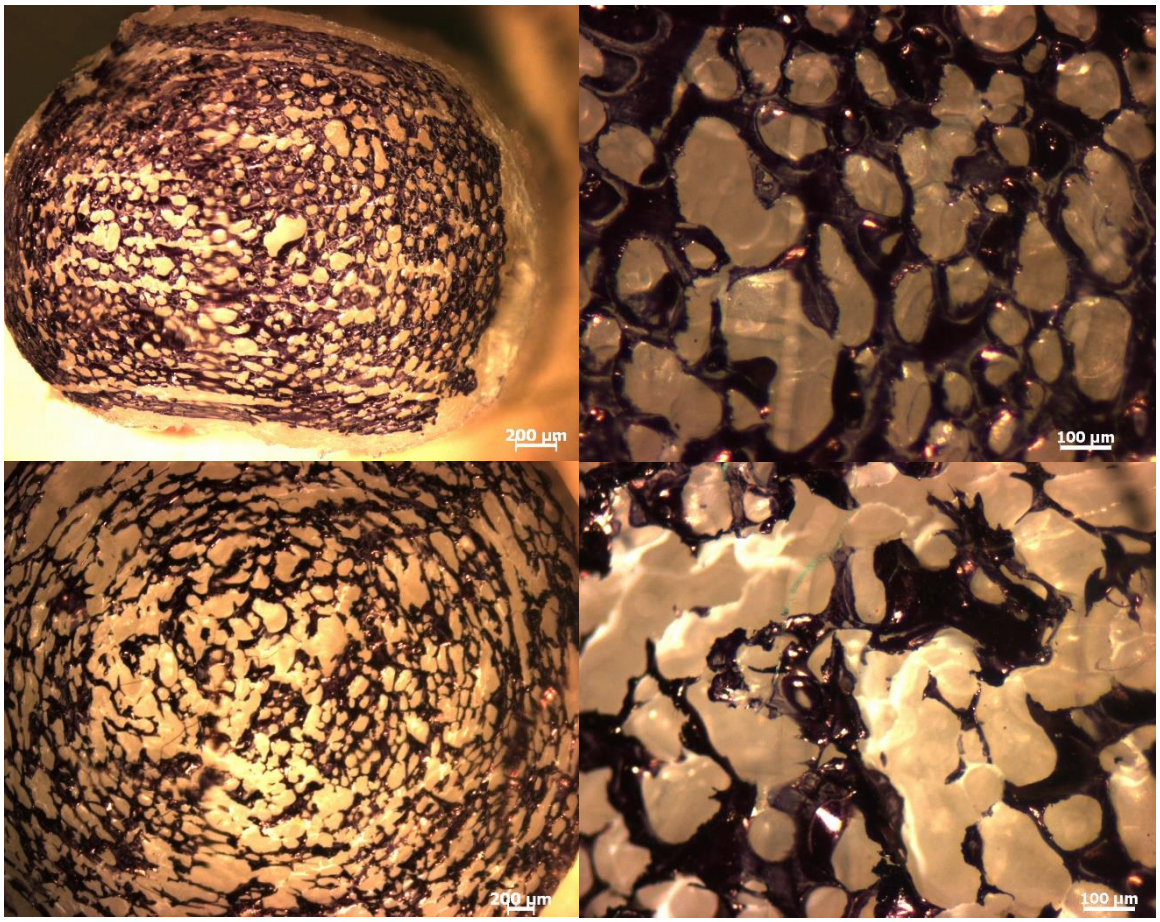

Figure 41: Micrographs of the LCB- PP foams; top: WB1, bottom: WB3

4.6.2 Foam morphology

The results of the foam morphology determination are given in Table 22.

Table 22: Mean cell density and mean cell diameter of the PP and LCB-PP foams

Sample Nr.	Mean cell density [cm^{-3}]	Variation coefficient [%]	Range R [cm^{-3}]	Mean cell diameter $\bar{d}$ [mm]	Standard deviation of the mean cell diameter [mm]
PP1	$1.62*10^{7}$	33.30	$1.71*10^{7}$	0.056	0.04
PP2	$2.45*10^{7}$	52.63	$3.82*10^{7}$	0.057	0.03
PP3	**$2.68*10^{7}$**	**36.45**	**$2.83*10^{7}$**	**0.035**	**0.01**
PP4	$9.90*10^{6}$	65.82	$1.68*10^{7}$	0.063	0.05
WB1	$1.46*10^{8}$	44.90	$1.62*10^{8}$	0.044	0.02
WB2	$5.28*10^{7}$	40.13	$6.64*10^{7}$	0.051	0.03
WB3	**$1.15*10^{7}$**	**50.72**	**$1.97*10^{7}$**	**0.096**	**0.10**
WB4	$4.22*10^{6}$	38.41	$5.04*10^{6}$	0.087	0.08
WBA	$8.75*10^{7}$	65.73	$1.55*10^{8}$	0.052	0.05
PP#PODIC	**$3.68*10^{7}$**	**30.36**	**$3.38*10^{7}$**	**0.059**	**0.04**

According to the set parameters (Table 21), the foam characteristics of the PP#PODIC must be compared to those of the sample PP3 and WB3 (highlighted in Table 22). The data in Table 22 shows that long chain branching of HC600TF did not improve the cell density much, but it must be noted that at die temperatures of above 135°C the cell density of LCB-PP and the linear PP are quite similar. The sample PP#PODIC had the highest cell density of all foams produced with this resin (HC600TF, PP series).

Figure 42 demonstrates the correlation between cell density and die temperature. It can be noted that the occurrence of cell coalescence at higher die temperatures lowers the cell density of LCB-PP significantly. This can be seen at the higher mean cell diameter of these samples. The cell density of linear PP is considerably lower than those of LCB-PP. The samples PP1 to PP3 show a rise of the cell density with higher temperature, but the high values of the variation coefficient should be noted. The sample PP4 had the highest die temperature and the lowest cell density of the linear PP foams. The best results of linear PP lie at 10^7 cm^{-3}, while those of LCB-PP reached 10^8 cm^{-3}.

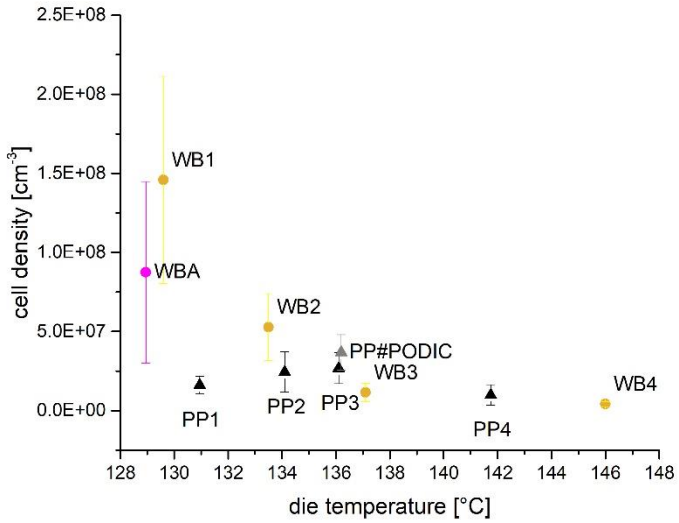

Figure 42: Cell density as a function of die temperature. Note the significantly lower cell density of linear PP compared to those of LCB-PP

The variation coefficient of the LCB-PP foams, that were extruded right above the crystallisation temperature, was relatively high. This is visualised in Figure 43.

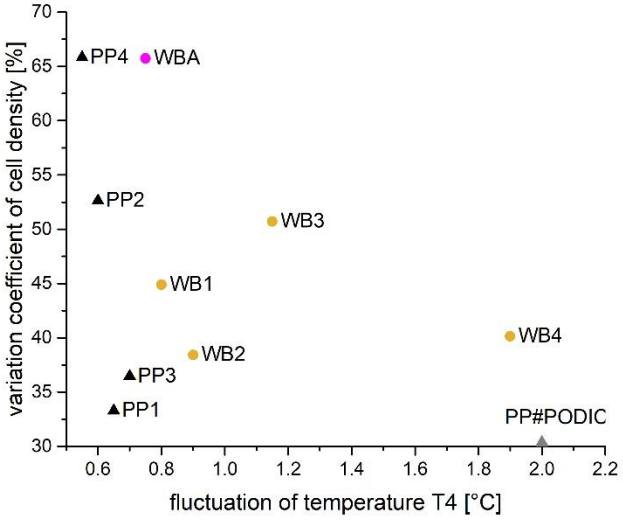

Figure 43: Correlation of the temperature and cell density fluctuation

The comparision of the variation coefficient of the cell density of linear PP and LCB-PP shows, that linear PP has a quite strong response to small temperature fluctuations. The variation coefficient of the cell density for LCB-PP was low over a larger range of temperature fluctuations. PP4 has the largest variation coefficient, which is not only promoted by the temperature fluctuations but also by the high die temperature itself.

Figure 43 shows, that the temperature fluctuations were only in the range of 2°C.

4.6.3 Foam density and compressive strength

The foam density and volume expansion ratio of the produced foams are given in Table 23.

Table 23: Foam density and volume expansion ratio of the PP and LCB-PP foams

Sample Nr.	Foam density [g/cm^3]	Standard deviation [g/cm^3]	Volume expansion ratio [-]
PP1	0.586	0.0128	1.56
PP2	0.566	0.0091	1.61
PP3	**0.596**	**0.0245**	**1.53**
PP4	0.672	0.0435	1.36
WB1	0.418	0.0061	2.12
WB2	0.407	0.0140	2.18
WB3	**0.363**	**0.0062**	**2.44**
WB4	0.374	0.0127	2.37
WBA	0.366	0.0014	2.55
PP#PODIC	**0.399**	**0.0400**	**2.29**

The foam density and volume expansion ratio of LCB-PP is better than those of linear PP. Long chain branching of HC600TF (PP#PODIC) successfully increased the volume expansion ratio.

In the processing guidelines for HMS PP published by Borealis AG [10] the foam density is listed between 250-600 kg/m^3 for a 30 mm single screw, flat die (Hydrocerol CT516 as nucleating agent, Hydrocerol CF40E as foaming agent). The design and process settings of the extruder as well as the blowing agent define the foam density and the quality of the produced foam. The given data can be taken as a guiding principle for the quality of the produced foams.

Due to the short strands, it was not possible to take enough samples from the produced linear polypropylene foams. The LCB-PP foams had overall a quite similar response under compressive load as the polyethylene foams. Although the compressive strength of the LCB-PP foams is higher than that of the polyethylene foams. The material behaviour under compressive load of LCB-PP foams is shown in Figure 44.

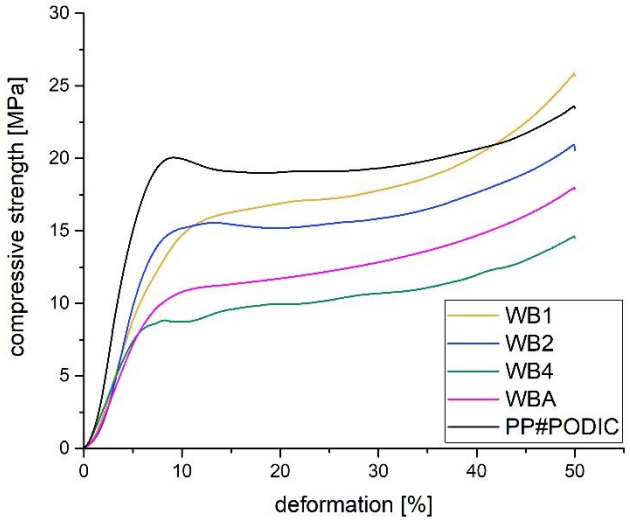

Figure 44: Compressive strength of LCB-PP foams

The foams of the WB series (WB135HMS, WB140HMS) have a rising compressive strength with rising foam density. This can be seen in Figure 45.

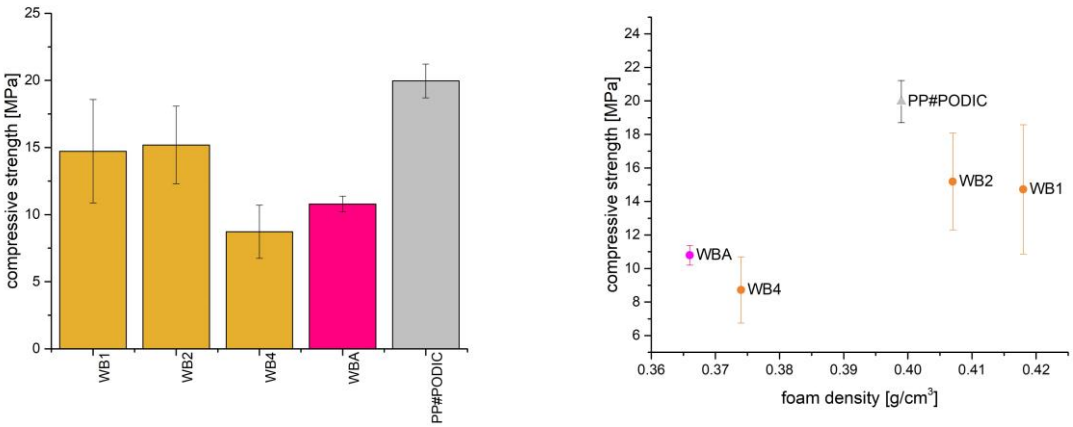

Figure 45: Compressive strength σ_{D10} (left) and compressive strength as a function of foam density (right)

The compressive strength of WB4 is lower compared to that of WB1 and WB2 due its more inhomogenic foam morphology which is a result of the set parameters. The compressive strength at 10% deformation is given in Table 24.

Table 24: Compression strength at 10% deformation for LCB-PP foams

Sample Nr.	σ_{D10} [MPa]	ε_{D10} [%]
WB1	14.72	10.0
WB2	15.19	10.0
WB4	8.72	10.0
WBA	10.79	10.0
PP#PODIC	19.96	10.0

4.6.4 Summary of linear and HMS- Polypropylene

The best results of linear PP an HMS-PP are given in Table 25.

Foam sample PP2 had a lower cell density as well as foam density than PP1, but PP1 did not show cell coalescence and had an overall more homogenic cell distribution. Both linear PP and HMS PP had a high variation of the cell diameter over the cross section of the foam.

The volume expansion ratio of HMS PP is higher and the foam density lower than those of LDPE. The cell density lies in the range of 10^7 cm^{-3} and 10^8 cm^{-3}. The results of PP#PODIC are as good as those received from the LCB-PP samples (WB-series).

Table 25: Properties of the best PP and LCB-PP foams

	PP1	**PP#PODIC**	**WB1**	**WBA**
Masterbatch	PEX 5024	PEX 5024	PEX 5024	PEX 5024
Die temperatureT4 [°C]	130.95	136.2	129.6	130.6
ΔT [°C]	31.25	54.5	43.85	42.2
Screw speed n [rpm]	27	27	27	27
Cell density [cm^{-3}]	$1.62*10^7$	$3.68*10^7$	$1.46*10^8$	$8.75*10^7$
Mean cell diameter [mm]	0.056	0.059	0.044	0.052
Foam density [g/cm^3]	0.586	0.399	0.418	0.366
Volume expansion ratio [-]	1.56	2.29	2.12	2.55
Compressive strength (at ε_{D10}) [MPa]	-	19.96	14.72	10.79

5 Comparison and discussion

The final physical properties of the thermoplastic foams are determined by the foam density, the cell size, the cell density and the volume expansion ratio. However, these parameters are not independent of each other [6].

5.1 Processing conditions and process variables

The set-up of the single screw extruder is sufficient for foaming of thermoplastics with acceptable foam quality. The quality of the produced foams varies over the length of the foam strand. This variation directly corresponds to the temperature control of the extruder. The temperature control of the section 3 and 4 is limited by the temperature in the melting section (S2). Temperature fluctuations during the foaming experiments affect the foam quality. The extent of the influence is measurable and can be reduced in future works by implementing a more effective temperature control in the die section.

From literature it is known that the die has a significant influence on the quality of the produced foams. The original die of the extruder has been extended with another forming section (T4). It has been shown in this thesis that the additional section improved the produced foams. The additional section allowed to further reduce the die temperature leading to a broader operating range at the die section. This had a significant effect on the quality of the foams.

The die temperature proofed to be the main parameter influencing the cell density as well as foam density. Polystyrene had the biggest processing window, a good foam quality could be achieved over a wide temperature range. Linear polypropylene had the smallest temperature range.

A high screw speed (40 rpm, 50 rpm) led to the formation of big gas bubbles and an inhomogenic cell distribution. The screw speed was consequently set to only 27 rpm.

The experiments with polystyrene have shown that the choice of chemical foaming agent is essential for the quality of the produced foam and the set processing conditions. The same chemical foaming agent (Hydrocerol PEX 5024) has been used to produce the polyethylene and polypropylene foams. With reference to the processing conditions for HMS-PP published by Borealis AG [10], the study of the impact of different chemical foaming agents could further improve the quality of the produced polypropylene foams. Moreover, the use of an additional masterbatch as nucleating agent is a promising approach for further investigations.

The set process parameters of the best foams for each thermoplastic as well as foam characteristics are listed in Table 26.

Table 26: Comparison of the properties of the best foams

	PE1	PP#PODIC	WB1	WBA	PS2A
Masterbatch	PEX 5024	PEX 5024	PEX 5024	PEX 5024	PEX 5040
Die temperature T4 [°C]	115.95	136.2	129.6	130.6	129.5
ΔT [°C]	26.4	54.5	43.85	42.2	36.7
Screw speed n [rpm]	27	27	27	27	27
Cell density [cm^{-3}]	$5.62*10^7$	$3.68*10^7$	$1.46*10^8$	$8.75*10^7$	$5.80*10^8$
Mean cell diameter [mm]	0.038	0.059	0.044	0.052	0.028
Foam density[g/cm^3]	0.506	0.399	0.418	0.366	0.320
Volume expansion ratio []	1.83	2.29	2.12	2.55	3.25
Compressive strength [MPa]	6	19.96	14.72	10.79	11.4

5.2 Foam morphology

The optimum cell density is always dependent on the cell diameter. The cell density decreases as the cell diameter rises. This is shown in Figure 46.

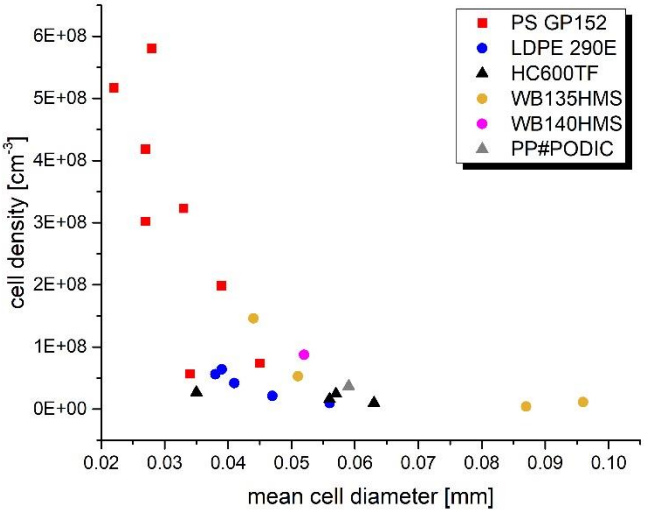

Figure 46: Cell density as a function of mean cell diameter.

As can be seen in Figure 47, the polystyrene foams had the highest mean cell density of all produced thermoplastic foams. The cell density of the two LCB-PP resins (WB135HMS, WB140HMS) lie between that of low-density polyethylene and polystyrene. The polypropylene foams had a poor cell density of only 10^6 cm^{-3} to 10^7 cm^{-3}. Polystyrene had the highest processing window and could be successfully foamed over a high temperature range.

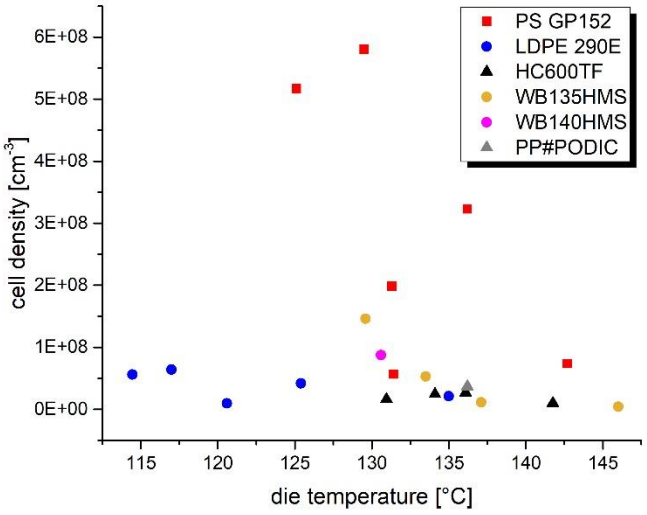

Figure 47: Cell density as a function of die temperature

5.3 Foam density and compressive strength

A low foam density alone is not a sufficient criterion for a good foam quality, because the formation of big gas bubbles reduces the foam density, but also leads to an inhomogeneous cell distribution. An inhomogeneous cell distribution has effect on the properties of the foam, like compressive strength. A low foam density and a high cell density are important indicators for a good foam quality. As can be seen in Figure 48, polystyrene foams had high cell density and consequently a low foam density.

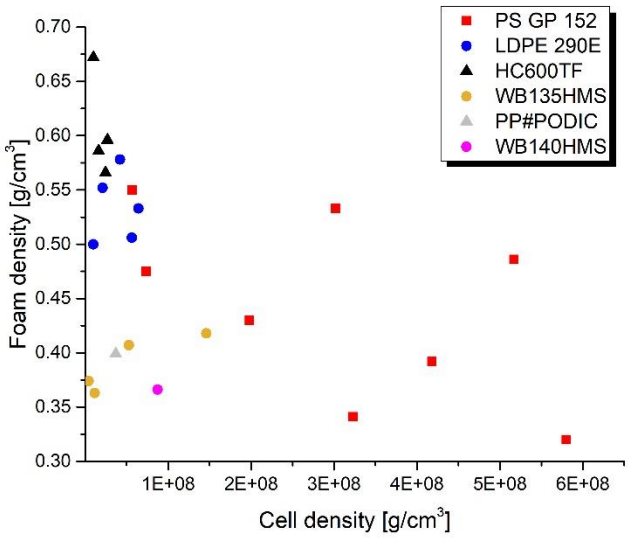

Figure 48: Foam density as function of cell density

The lowest foam density was reached by the polystyrene foams, followed by those of the LCB-PP foams. The cell density of polystyrene and LCB-PP was higher than those of low-density

polyethylene and linear polypropylene. The polypropylene foams had due to their low cell density also a high foam density. The foam density as a function of die temperature is given in Figure 49.

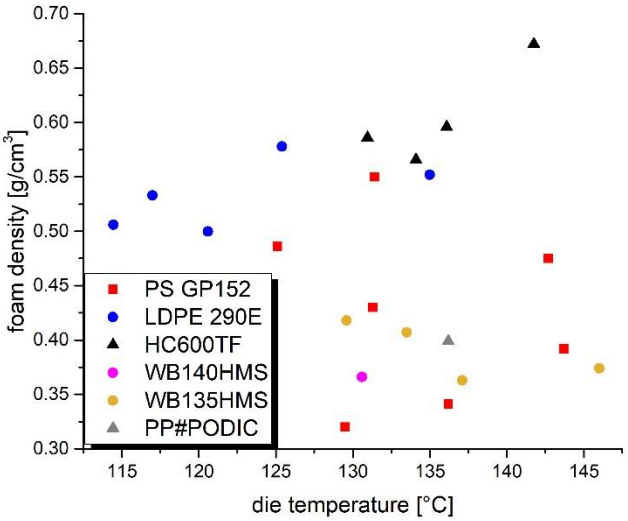

Figure 49: Foam density as a function of die temperature

Extrusion foaming of long chain branched polypropylene leads to a lower foam density, a higher volume expansion ratio and a more homogeneous cell structure compared to linear polypropylene. It can be seen in Figure 49, that the foam density of LCB-PP foams is significantly lower than that of linear PP foams. Reactive extrusion with PODIC combined with extrusion foaming has proofed to be a good method to produce polypropylene foams. It should be noted that the achieved volume expansion ratio as well as the foam density of foams produced with chemical blowing agents is significantly lower than those of physical blowing agents.

The material behaviour under compressive load depends on various factors, therefore a homogeneous foam morphology is essential. Unfortunately, the foam morphology over the length of the foam strand varied due to temperature fluctuations at the die. The foam samples of the polyethylene strands showed a quite similar material behaviour under compressive load due to their pretty homogeneous cell density and cell distribution over the cross section. This was not given for the polystyrene foams, which also had cell coalescence and an inhomogeneous cell distribution due to bigger gas bubbles.

Figure 50 compares the different material behaviour under compressive load for the best samples of the produced thermoplastic foams. The polyethylene foam PE1 has the lowest compressive strength, while PP#PODIC has the highest. This can also be seen in Figure 51.

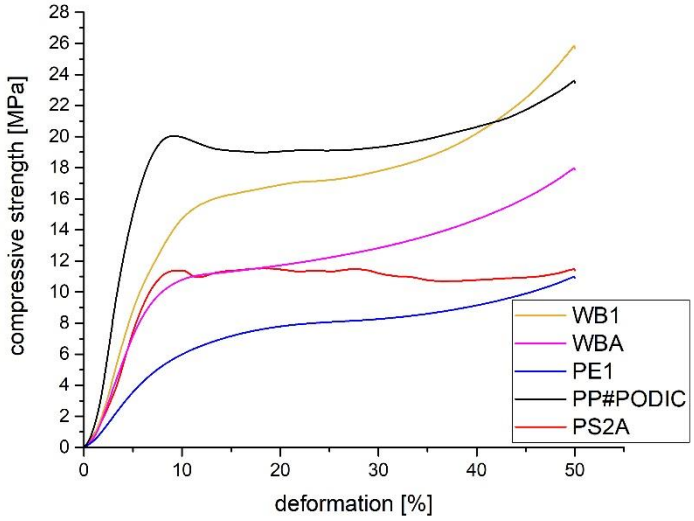

Figure 50: Comparison of the material behaviour under compressive load for different thermoplastic foams

The polyethylene foam PE1 had the most homogeneous foam morphology due to its low variation coefficient of the cell density compared to the other samples, especially to that of WB1 and PS2A. This contributes to the low compressive strength of the polyethylene foam. The higher variation coefficient of the cell density of the other foams reduces the foam density. The low cell density of the foam sample PP#PODIC leads to its high compressive strength. The better compressive strength of PP compared to PS is one of the advantages that make PP foams a promising substitute in industrial applications.

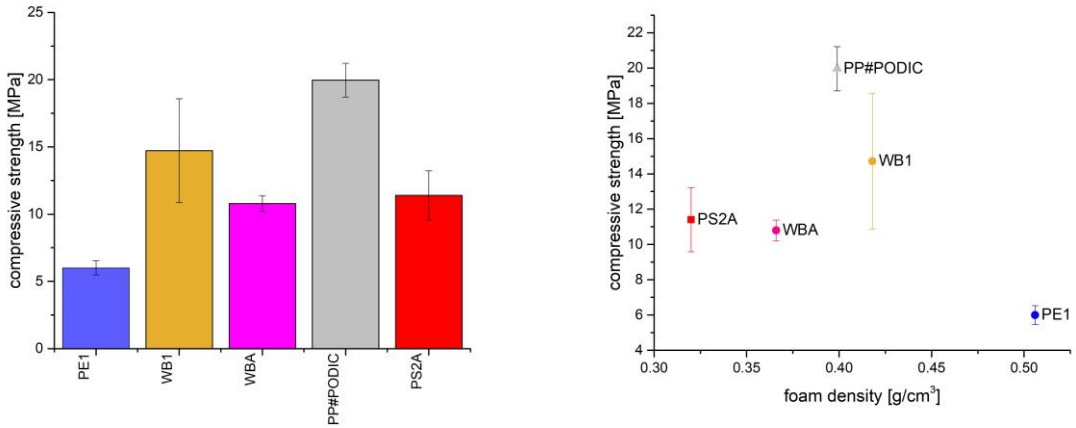

Figure 51: Compressive strength of the best foam samples (left) and compressive strength as a function of foam density (right)

6 Conclusion and future work perspective

The three main questions of this master thesis were:

- Which processing conditions and process variables have an influence on the extrusion foaming of thermoplastics?
- What determines the foamability of selected thermoplastic resins?
- What is the impact of long-chain branching of polypropylene on its foamability?

In order to answer these questions, it was necessary to evaluate the suitability of the single-screw extrusion set-up first. Chemical foaming was determined as promising approach for extrusion foaming. The original extrusion set-up was modified by adding an additional forming section (S4).

On basis of comprehensive literature study and foaming experiments with polystyrene it was possible to determine important processing conditions. The experiments have shown that the die temperature as well as the screw speed are the main parameters that influence a foam process. The quality of the produced foams was significantly improved due to broader operation range of the temperature at the die section. The choice of foaming agent also affects the quality of the produced foam.

Lacking temperature control in the die section resulted in temperature fluctuation that affected the cell density. Consequently, it was necessary to measure the temperature fluctuation and estimate the influence on the cell density. Future work could focus on improving the temperature control of the single screw extruder and the construction of a die with optimum pressure drop rate to further improve the foam quality.

First an easy-to-foam material with a broad processing window was studied, then the foamability of semi-crystalline polyethylene with a narrower processing window was investigated. The obtained insight from previous foam processes was then used for the foaming of polypropylene. In total three thermoplastics with different processing windows were analysed. Rheological measurements were performed to determine the rheological properties of the used thermoplastics and their effect on the foamability. It was found that high melt strength and pronounced strain hardening are important properties for a good foamability.

Linear PP as well as commercially traded HMS-PP were foamed with a CBA to analyse the impact of long-chain branching on the foamability of PP. The volume expansion ratio and the cell density of the linear PP foam was significantly lower than those of the HMS-PP. The effect of long- chain branching was investigated more in detail by reactive extrusion of linear PP with PODIC. In addition, a CBA was added to foam the polypropylene in one step. The results of the characterisation of this foam showed that the quality was as good as those of other HMS-PP foams. Consequently, this approach is a promising method to produce good quality foams from linear PP resins.

Future work could focus on further improving the foam characteristics, such as volume expansion ratio or cell density. This could be conducted by using physical foaming agents or investigating the effect of different chemical foaming agents on the foam quality. The use of nucleation agents is also a promising approach in this context.

The obtained results and the gained knowledge in the field of extrusion foaming with CBA should contribute to further work in the project “innovative polymer recycling”. Future work will focus on foaming of polypropylene from post-consumer waste with PODIC and CBA.

7 Bibliography

[1] Kamleitner, F., Duscher, B., Koch, T., Knaus, S., Schmid, K. and Archodoulaki, V.-M. (2017) 'Influence of the Molar Mass on Long-Chain Branching of Polypropylene', *Polymers*, 9(9), pp. 442.

[2] Kamleitner, F., Duscher, B., Koch, T., Knaus, S. and Archodoulaki, V.-M. (2017) 'Long chain branching as an innovative up-cycling process of polypropylene post-consumer waste – Possibilities and limitations', *Waste Management*, 68(Supplement C), pp. 32-37.

[3] Lee, S. T. (2000) *Foam Extrusion: Principles and Practice.* CRC Press.

[4] Technavio (Jan 2017) *Global Polymer Foam Market 2017-2021* (IRTNTR11120, (Accessed: 21.11.2017).

[5] Nam, G. J., Yoo, J. H. and Lee, J. W. (2005) 'Effect of long-chain branches of polypropylene on rheological properties and foam-extrusion performances', *Journal of Applied Polymer Science*, 96(5), pp. 1793-1800.

[6] Xu, X., Park, C. B., Xu, D. and Pop-Iliev, R. (2003) 'Effects of die geometry on cell nucleation of PS foams blown with CO2', *Polymer Engineering & Science*, 43(7), pp. 1378-1390.

[7] marketsandmarkets.com (November 2017) *Polymer Foam Market by Type (PU, PS, PO, PVC, Phenolic, Melamine), End-Use Industry (Building&Construction, Packaging, Automotive, Furniture & Bedding, Footware, Sports & Recreational), and Region - Global Forecast to 2022* (CH 1465. Available at: https://www.marketsandmarkets.com/Market-Reports/foams-market-1011.html (Accessed: 21.11.2017).

[8] Naguib, H. E., Park, C. B., Panzer, U. and Reichelt, N. (2002) 'Strategies for achieving ultra low-density polypropylene foams', *Polymer Engineering & Science*, 42(7), pp. 1481-1492.

[9] PlasticsEurope (2016) 'Plastics - the Facts 2016', *PlasticsEurope - Association of Plastics Manufacturers*.

[10] Borealis AG, B. P. L. (2016) 'Daploy High-Melt-Strength PP'.

[11] Wypych, G. (2017) *Handbook of Foaming and Blowing Agents.* Elsevier Science.

[12] Xu, Z.-M., Jiang, X.-L., Liu, T., Hu, G.-H., Zhao, L., Zhu, Z.-N. and Yuan, W.-K. (2007) 'Foaming of polypropylene with supercritical carbon dioxide', *The Journal of Supercritical Fluids*, 41(2), pp. 299-310.

[13] Klempner, D., Sendijarevi′c, V. and Aseeva, R. M. (2004) *Handbook of Polymeric Foams and Foam Technology*. Hanser Publishers, p. 507ff.

[14] Park, C. B. and Cheung, L. K. (1997) 'A study of cell nucleation in the extrusion of polypropylene foams', *Polymer Engineering & Science*, 37(1), pp. 1-10.

[15] Park, C. B., Behravesh, A. H. and Venter, R. D. (1997) 'A Strategy for the Suppression of Cell Coalescence in the Extrusion of Microcellular High-Impact Polystyrene Foams', *Polymeric Foams: Vol. 669 ACS Symposium Series*: American Chemical Society, pp. 115-129.

[16] Lee, C. H., Lee, K.-J., Jeong, H. G. and Kim, S. W. (2000) 'Growth of gas bubbles in the foam extrusion process', *Advances in Polymer Technology*, 19(2), pp. 1098-2329.

[17] *Foam Extrusion-53.* (2013): Elsevier Inc.

[18] Stange, J., Uhl, C. and Münstedt, H. (2005) 'Rheological behavior of blends from a linear and a long-chain branched polypropylene', *Journal of Rheology*, 49(5), pp. 1059-1079.

[19] Menges, G., Haberstroh, E., Michaeli, W. and Schmachtenberg, E. (2011) *Menges Werkstoffkunde Kunststoffe.* Hanser.

[20] Bonnet, M. (2013) *Kunststofftechnik: Grundlagen, Verarbeitung, Werkstoffauswahl und Fallbeispiele.* Springer Fachmedien Wiesbaden.
[21] GmbH, I. Available at: http://iwi-gmbh.com/iwi/pdf/IWI_EPS_en.pdf (Accessed 09.11.2017).
[22] GmbH., S. H. (2017) 'Herstellen von Polyurethan- Schaumstoffen ohne Treibmittel'. Available at: https://www.schaumstoffehelgers.de/news/schaumstoffe-treibmittelfrei.html (Accessed 09.11.2017).
[23] Wintermantel, E. and Ha, S. W. (2009) *Medizintechnik: Life Science Engineering.* Springer Berlin Heidelberg.
[24] Klempner, D., Sendijarevi′c, V. and Aseeva, R. M. (2004) *Handbook of Polymeric Foams and Foam Technology*. Hanser Publishers, p. 507ff.
[25] Pollock, W. C., Grossman, S. A. and Owens, A. H. 2010. Polymeric drug delivery systems and thermoplastic extrusion processes for producing such systems. Google Patents.
[26] Eyerer, P., Hirth, T. and Elsner, P. (2008) *Polymer Engineering: Technologien und Praxis.* Springer Berlin Heidelberg, p. 296-299.
[27] Naguib, H. E., Wang, J., Park, C. B., Mukhopadhyay, A. and Reichelt, N. (2003) 'Effect of recycling on the rheological properties and foaming behaviors of branched polypropylene', *Cellular Polymers,* 22(1), pp. 1-22.
[28] Eaves, D. (2004) *Handbook of Polymer Foams.* Rapra Technology, p. 28-33.
[29] Klempner, D., Sendijarevi′c, V. and Aseeva, R. M. (2004) *Handbook of Polymeric Foams and Foam Technology*. Hanser Publishers, p. 5ff.
[30] Eaves, D. (2004) *Handbook of Polymer Foams.* Rapra Technology, p. 28.
[31] Domininghaus, H., Elsner, P., Eyerer, P. and Hirth, T. (2008) *DOMININGHAUS - Kunststoffe: Eigenschaften und Anwendungen.* Springer Berlin Heidelberg.
[32] Sauceau, M., Nikitine, C., Rodier, E. and Fages, J. (2007) 'Effect of supercritical carbon dioxide on polystyrene extrusion', *The Journal of Supercritical Fluids,* 43(2), pp. 367-373.
[33] Ma, C.-Y. and Han, C. D. (1983) 'Foam extrusion characteristics of thermoplastic resin with fluorocarbon blowing agent. II. Polystyrene foam extrusion', *Journal of Applied Polymer Science,* 28(9), pp. 2983-2998.
[34] Kundu, D. 2017. High temperature non-crosslinked polyethylene-based foam and method of making the same. Google Patents.
[35] Wagner, J. R. 2014. *RE: Extrusion, 2nd ed.* Type to Giles Jr, H.F., Giles, H.F. & Mount, E.M.
[36] 'Rheological properties and foaming behavior of polypropylenes with different molecular structures', (2006) *Journal of Rheology,* 50(6), pp. 907-923.
[37] Gotsis, A. D., Zeevenhoven, B. L. F. and Hogt, A. H. (2004) 'The effect of long chain branching on the processability of polypropylene in thermoforming', *Polymer Engineering & Science,* 44(5), pp. 973-982.
[38] Lagendijk, R. P., Hogt, A. H., Buijtenhuijs, A. and Gotsis, A. D. (2001) 'Peroxydicarbonate modification of polypropylene and extensional flow properties', *Polymer,* 42(25), pp. 10035-10043.
[39] Gahleitner, M. (2001) 'Melt Rheology of Polyolefins', 26, pp. 895-944.
[40] Klempner, D., Sendijarevi′c, V. and Aseeva, R. M. (2004) *Handbook of Polymeric Foams and Foam Technology*. Hanser Publishers, p. 234-262.
[41] Wagner Jr, J. R., Mount Iii, E. M. and Giles Jr, H. F. (2014) '20 - Polymer Rheology', *Extrusion (Second Edition).* Oxford: William Andrew Publishing, pp. 233-240.
[42] Mezger, T. (2010) *Das Rheologie-Handbuch: für Anwender von Rotations- und Oszillations-Rheometern.* Vincentz Network.

[43] Münstedt, H., Kurzbeck, S. and Stange, J. (2006) 'Advances in Film Blowing, Thermoforming, and Foaming by Using Long-Chain Branched Polymers', *Macromolecular Symposia*, 245-246(1), pp. 181-190.

[44] Han, X., Koelling, K. W., Tomasko, D. L. and Lee, L. J. (2002) 'Continuous microcellular polystyrene foam extrusion with supercritical CO2', *Polymer Engineering & Science*, 42(11), pp. 2094-2106.

[45] Wypych, G. (2017) *Handbook of Foaming and Blowing Agents.* Elsevier Science.

[46] Lee, P. C., Kaewmesri, W., Wang, J., Park, C. B., Pumchusak, J., Folland, R. and Praller, A. (2008) 'Effect of die geometry on foaming behaviors of high-melt-strength polypropylene with CO2', *Journal of Applied Polymer Science*, 109(5), pp. 3122-3132.

[47] Naguib, H. E., Park, C. B. and Reichelt, N. (2004) 'Fundamental foaming mechanisms governing the volume expansion of extruded polypropylene foams', *Journal of Applied Polymer Science*, 91(4), pp. 2661-2668.

[48] Wypych, G. (2017) *Handbook of Foaming and Blowing Agents.* Elsevier Science, p. 45-49

[49] *DIN EN ISO 11357-1:2016 Kunststoffe-Dynamische Differenz-Thermoanalyse (DSC)-Teil 1:Allgemeine Grundlagen (ISO 11357-1:2016).*

[50] *DIN EN ISO 11357-3 Kunststoffe-Dynamische Differenz Thermoanalyse (DSC)- Teil 3: Bestimmung der Schmelz-und Kristallisationstemperatur und der Schmelz- und Kistrallisationsenthalpie (ISO/DIS 11357-3:2017).*

[51] *DIN EN ISO 11358-1 Kunststoffe- Thermogravimetrie (TG) von Polymeren - Teil 1: Allgemeine Grundsätze (ISO 11358-2:2014).*

[52] *DIN EN ISO 844 Harte Schaumstoffe - Bestimmung der Druckeigenschaften (ISO 844:2014).*

[53] Spitael, P. and Macosko, C. W. (2004) 'Strain hardening in polypropylenes and its role in extrusion foaming', *Polymer Engineering & Science*, 44(11), pp. 2090-2100.

[54] Zoppoth, S. (2017) *Upcycling von Polypropylen: Herstellung von Schäumen. Upcycling von Polypropylene: foaming* Wien: Wien.

[55] Papula, L. (2011) *Mathematik für Ingenieure und Naturwissenschaftler Band 3: Vektoranalysis, Wahrscheinlichkeitsrechnung, Mathematische Statistik, Fehler- und Ausgleichsrechnung.* Vieweg+Teubner Verlag.

[56] Park, C. B., Baldwin, D. F. and Suh, N. P. (1995) 'Effect of the pressure drop rate on cell nucleation in continuous processing of microcellular polymers', *Polymer Engineering & Science*, 35(5), pp. 432-440.

8 List of figures

9 List of tables

10 Notation

Abbreviations

aPP	atactic polypropylene
CAGR	Compound annual growth rate [%]
CBA	chemical blowing agent
T4	Die temperature [°C]
DSC	Differential scanning calorimetry
EPE	expanded polyethylene
EPP	expanded polypropylene
EPS	expanded polystyrene
T1	Feed temperature [°C]
HMS	high melt strength
HMS-PP	high melt strength polypropylene
PE-HD / HD-PE	high-density polyethylene
iPP	isotactic polypropylene
LLDPE	linear low-density polyethylene
LCB	long chain branched
LCB-PP	long chain branched polypropylene
PE-LD / LD-PE	low-density polyethylene
MFI	melt flow index [Volume/10min]
T2	melting temperature [°C]
Nr.	number
PODIC	peroxydicarbonates
PBA	physical blowing agent
PP	polypropylene
PS	polystyrene
PU	polyurethane
n	Screw speed [rpm]
S1	section 1 (feeding section)
S2	section 2 (melting + compression section)
S3	section 3 (metering section)
S4	section 4 (forming section)
SPP	syndiotactic polypropylene
T3	Temperature in section 3 [°C]
TGA	Thermogravimetric analysis
TR	Trouton's ratio

Symbols

A	area [m^2]
CH_3	methyl group
CO_2	carbon dioxide
d	average diameter [m]
d_i	diameter of cell i-type [m]
G_P	plateau modulus [Pa]
G‘	Storage modulus [Pa]
G‘‘	Loss modulus [Pa]
G	buoyancy [g]
M	magnification of the microscope [-]
N_0	cell density [m^{-3}]
N_2	nitrogen
n	number of cells in A [-]
n_i	number of cell i-type [-]
p	pressure [MPa]
R	range
r	correlation coefficient
s	standard deviation
T	Temperature [°C]
T_G	glass transition temperature [°C]
T_m	melting temperature [°C]
t	time [s]
V_a	volume expansion ratio [-]
V_f	void fraction [-]
$W(a)$	weight of sample in air [g]
$\bar{x}$	arithmetic mean
x_i	measured values
x_{max}	maximum value
x_{min}	minimum value
$Cov(X,Y)$	covariance
$\dot{\gamma}$	strain rate [s^{-1}]
ε_{dB}	deformation at compressive yield strength [%]
ε_{D10}	10% deformation [%]
η	Viscosity [Pa*s]
η_E^+	extensional viscosity [Pa*s]
η^0	zero viscosity [Pa*s]
η^*	complex viscosity [Pa*s]
v	coefficient of variation
ρ	density [g/cm^3]
ρ_f	foam density [g/cm^3]
ρ_p	density of unexpanded polymer [g/cm^3]
ρ_w	density of water [g/cm^3]
σ_{dB}	yield strength [MPa]
σ_{D10}	compressive strength at 10% deformation [MPa]
ω	frequency [rad/s]

11 Appendix

Rheology of the thermoplastic resins

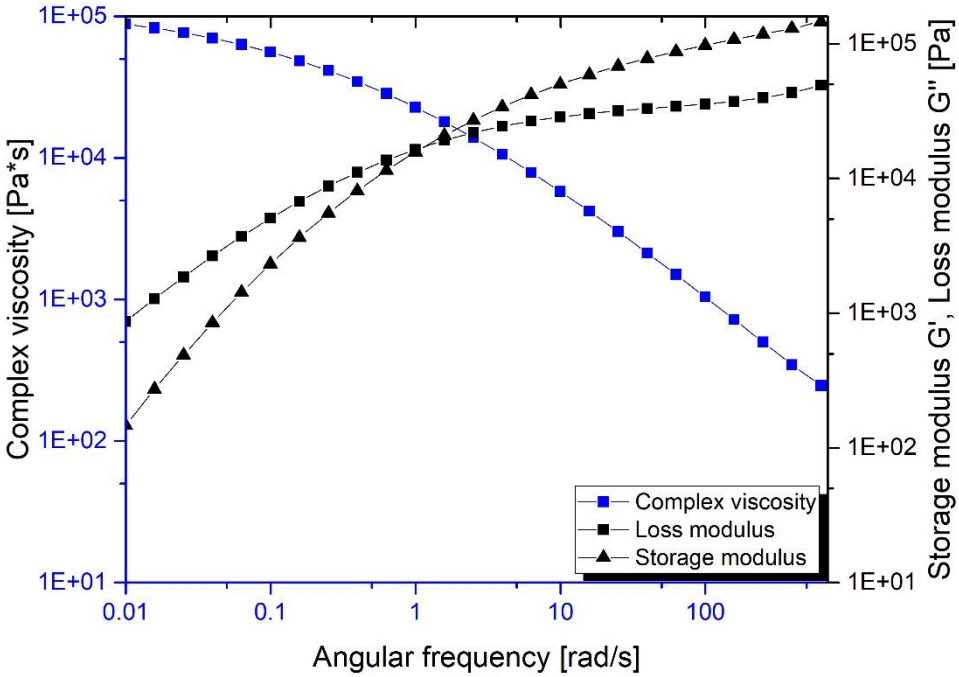

Figure 52: Polystyrene PS GP152

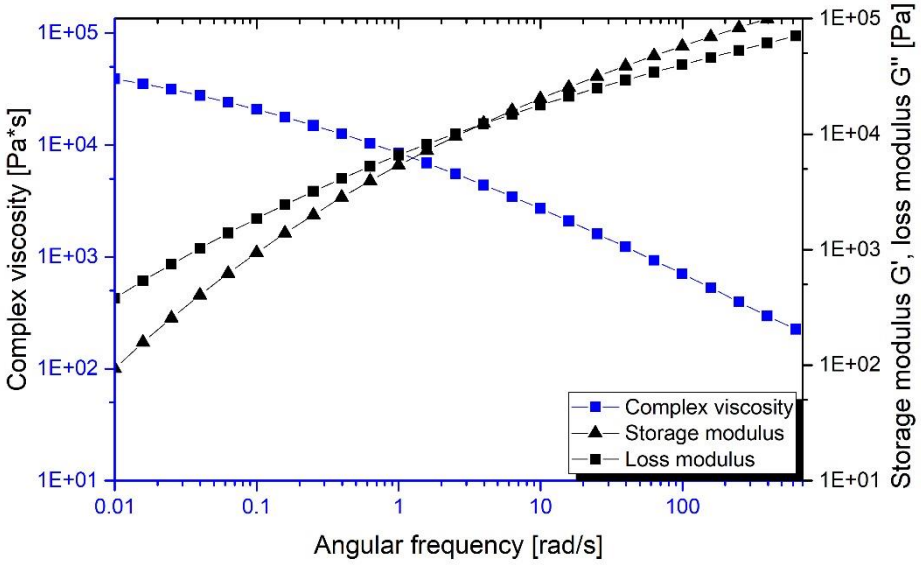

Figure 53: LDPE 290E

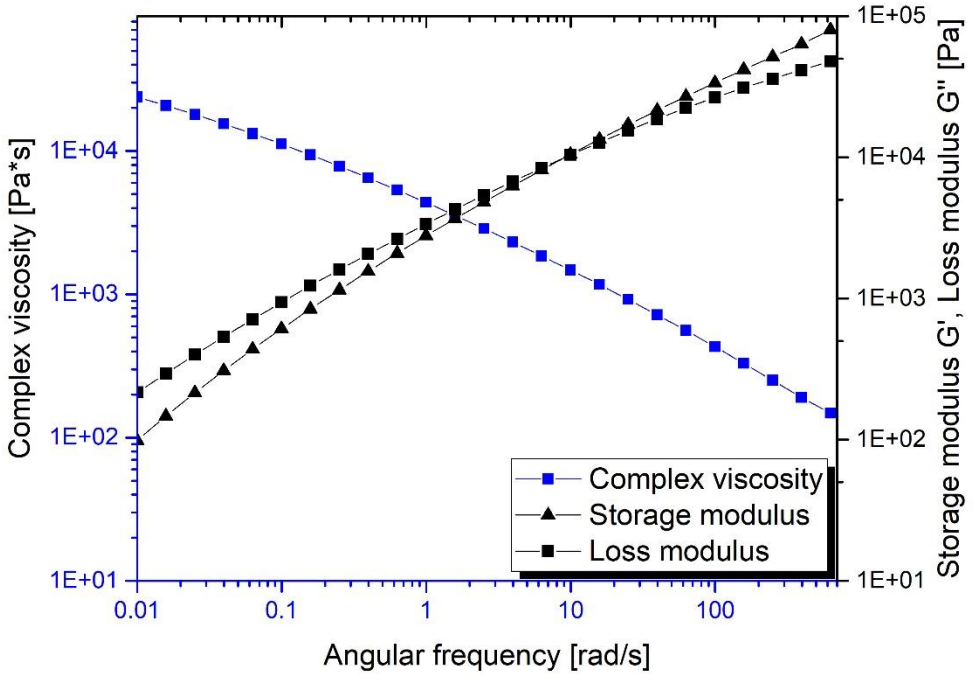

Figure 54: WB135HMS

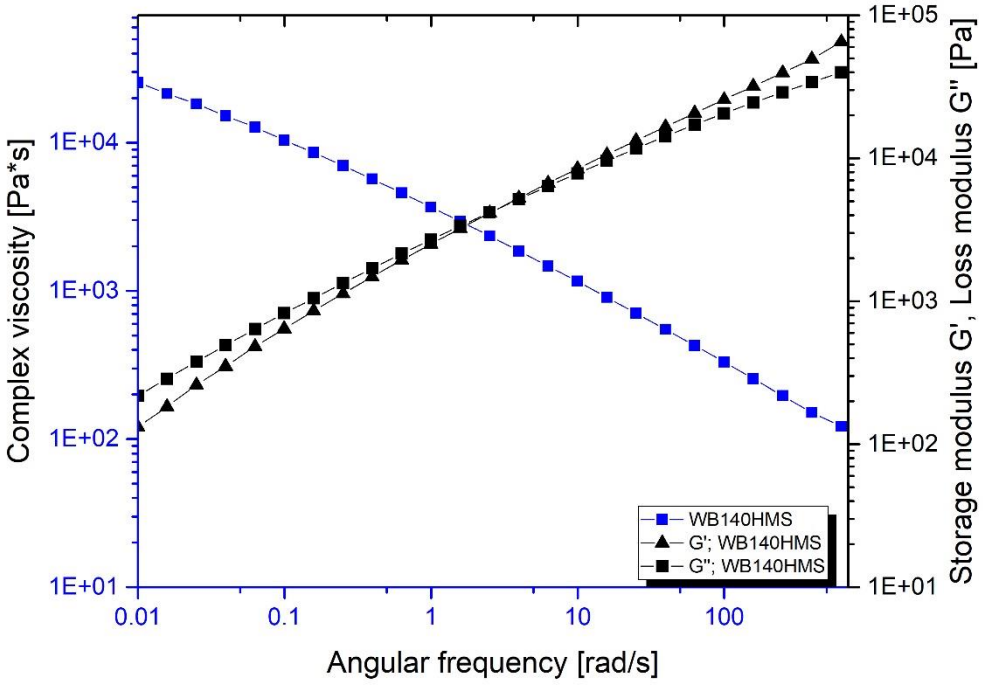

Figure 55: WB140HMS

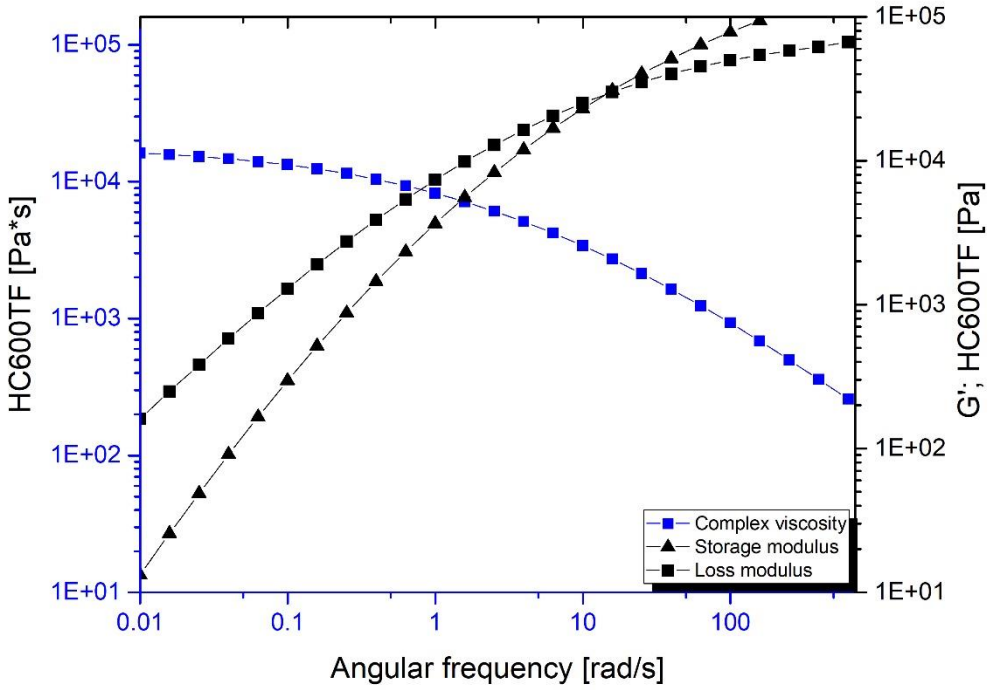

Figure 56: HC600TF